RoMa: A Robust Model Watermarking Scheme for Protecting IP in Diffusion Models

Yingsha Xie[1,2], Rui Min[3], Zeyu Qin[3], Fei Ma[2], Li Shen[1,2,4]*, Fei Yu[2], Xiaochun Cao[1]
[1]School of Cyber Science and Technology, Shenzhen Campus of Sun Yat-sen University, China
[2]Guangdong Laboratory of Artificial Intelligence and Digital Economy (SZ), China
[3]Hong Kong University of Science and Technology, China
[4]Center for AI Theoretical Foundation and Systems, Shenzhen Loop Area Institute, China
xieysh26@mail2.sysu.edu.cn, mathshenli@gmail.com

Abstract

Preserving intellectual property (IP) within a pre-trained diffusion model is critical for protecting the model's copyright and preventing unauthorized model deployment. In this regard, model watermarking is a common practice for IP protection that embeds traceable information within models and allows for further verification. Nevertheless, existing watermarking schemes often face challenges due to their vulnerability to fine-tuning, limiting their practical application in general pre-training and fine-tuning paradigms. Inspired by using mode connectivity to analyze model performance between a pair of connected models, we investigate watermark vulnerability by leveraging Linear Mode Connectivity (LMC) as a proxy to analyze the fine-tuning dynamics of watermark performance. Our results show that existing watermarked models tend to converge to sharp minima in the loss landscape, thus making them vulnerable to fine-tuning. To tackle this challenge, we propose RoMa, a **Ro**bust **M**odel w**a**termarking scheme that improves the robustness of watermarks against fine-tuning. Specifically, RoMa decomposes watermarking into two components, including *Embedding Functionality*, which preserves reliable watermark detection capability, and *Path-specific Smoothness*, which enhances the smoothness along the watermark-connected path to improve robustness. Extensive experiments on benchmark datasets MS-COCO-2017 and CUB-200-2011 demonstrate that RoMa significantly improves watermark robustness against fine-tuning while maintaining generation quality, outperforming baselines. The code is available at https://github.com/xiekks/RoMa.

1 Introduction

Diffusion models [20, 19, 52, 45] have demonstrated significant advancements across various generative fields [22, 61, 73, 6], which are largely driven by the widespread practice of fine-tuning pre-trained models [67, 47]. While pre-trained diffusion models are the foundation of many applications, training them typically necessitates millions of high-quality training images [50] as well as significant computational resources [54]. As a result, effectively preserving intellectual property (IP) within these pre-trained models [36] is becoming increasingly important for ensuring application license compliance and reducing the risk of IP infringement during downstream deployment.

In this literature, model watermarking [72, 63, 13, 26, 28, 7, 58, 12] has proven to be a common and effective practice for protecting the IP within a diffusion model. By embedding traceable information within the model weights, the detector can leverage a predefined detection mechanism for further

*Correspondence to: Li Shen <mathshenli@gmail.com>.

39th Conference on Neural Information Processing Systems (NeurIPS 2025).

verification. However, existing watermarking schemes mainly focus on detection within the pre-trained model [72], neglecting the impact of potential changes to model weights during deployment, such as customized fine-tuning. This oversight leads to a significant vulnerability in these schemes, as watermark detection becomes less effective after model fine-tuning [28, 58], limiting their practical application in real-world scenarios.

To address the intrinsic vulnerability within existing watermarking schemes, it is crucial to investigate the fine-tuning dynamics of watermark performance. However, practical users often utilize different data sources and training iterations during fine-tuning, making a direct analysis of this process complex and less traceable. Inspired by previous work [18, 15, 37] using mode connectivity to explore the impact of parameter change along a model connected path, we instead use the mode connectivity path as a proxy to analyze robustness performance during model fine-tuning. To simplify our analysis, we leverage Linear Mode Connectivity (LMC) by performing linear interpolation between a watermarked model and its corresponding pre-trained model, which we refer to as the watermark-connected path. Preliminary results shown in Fig. 2 reveal that existing watermarking schemes suffer from a significant drop in watermark quality, even with a large interpolation coefficient (e.g., $t = 0.9$). These findings are consistent with their robustness vulnerability against model fine-tuning [28, 58], where only a few fine-tuning steps can effectively remove the embedded watermarks. On the other hand, directly applying existing smoothness-aware optimization, such as SAM [14] and PGN [71], does not introduce robustness improvement along the watermark-connected path, emphasizing the importance of preserving the *path-specific smoothness*. Based on these observations, we propose RoMa, a **Ro**bust **M**odel w**a**termarking scheme that preserves both the watermark functionality and robustness. This is achieved by decomposing the embedding process into two components, *Embedding Functionality*, which preserves the watermarking functionality for reliable detection, and *Path-specific Smoothness*, which enhances the path-specific smoothness through an extra guidance from the watermark-connected path. Our demos in Fig. 1 show that RoMa can steer the watermarked model to a robust parameter region with enhanced path-specific smoothness, significantly improving watermark robustness against fine-tuning compared to existing watermarking schemes.

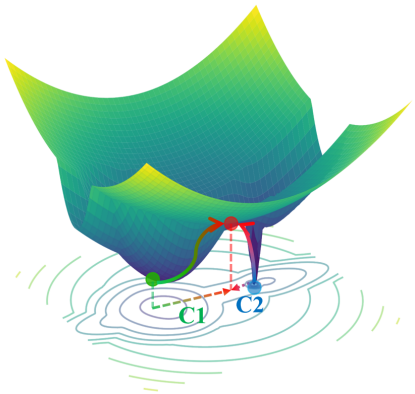

Figure 1: Watermark loss landscape visualization. The red point represents the originally pre-trained model with high watermark loss, the blue point represents models obtained by existing watermarking schemes, and the green point represents models optimized with RoMa. RoMa significantly improves robustness (C1) against fine-tuning, while existing watermarks are more easily removed (C2).

To thoroughly evaluate the effectiveness of RoMa, we conduct extensive experiments on MS-COCO-2017 and CUB-200-2011 datasets against four widely adopted evaluation metrics [70]: Robustness, Quality, Detectability, and Security, as detailed in Section 5.2. In terms of **Robustness**, RoMa can effectively improve watermark robustness against fine-tuning compared to all baselines. Specifically, RoMa maintains detectable watermark performance over 4,000 fine-tuning steps, whereas WatermarkDM loses verifiability after approximately 1,000 steps; In terms of **Quality**, RoMa preserves a high generation capability compared to the pre-trained diffusion model with a marginal drop in quality metrics; In terms of **Detectability**, RoMa maintains reliable watermark verification with AUC=1; In terms of **Security**, RoMa demonstrates significantly enhanced resistance against adaptive attacks. Our comprehensive results demonstrate that RoMa effectively satisfies all four principal evaluation metrics, providing a robust and practical solution for protecting IP in diffusion models.

2 Related Work

Model Watermarking for Diffusion Models. Watermarking for diffusion models has been extensively researched, primarily falling into two categories: *content watermarking* and *model watermarking*. Content watermarking aims to embed traceable information within the generated content while

preserving the original semantic structure. Techniques from traditional watermarking, such as DCT & DWT [4, 17] and deep-learning based schemes [75, 55] can be directly applied to integrate watermarks into images in a post-hoc manner. Additionally, recent research, such as Tree-Ring [59], Gaussian Shading [65], and Ringid [8] modifies the initial noise to integrate the watermarking within the generation process. Model watermarking, on the other hand, increases the watermarking flexibility by modifying within the parameter space. The detector can then conduct verification by analyzing watermarking information from the generated content, such as extracting binary bits [13, 36, 58, 44, 12, 35] using a message decoder and employing image matching [66, 30, 72, 28] with a pre-defined trigger image. Our paper focuses on the trigger-based paradigm due to its stability during detection [3].

Linear Mode Connectivity. Mode connectivity [10, 18, 33] was initially introduced to explore the conjecture that the loss minima of different Deep Neural Networks (DNNs) can be linked by low-loss curves. While connecting two separately trained models typically involves complex path construction, a simplified form named Linear Mode Connectivity (LMC) [15, 11, 1, 37, 74, 24] can be directly applied to analyze the connectivity between models fine-tuned from the same initialization. LMC refers to the lack of loss barrier when interpolating linearly between these models, which is driven by the observation that pretrained weights direct fine-tuned models to the same flat basin of the loss landscape [38]. Inspired by [18, 15, 38, 37], we utilize LMC as a proxy to examine the fine-tuning dynamics of watermark performance.

Watermark Robustness against Fine-tuning. In line with our research, two related works, including AIAO [28] and SleeperMark [58], also explored the watermark robustness against model fine-tuning. Specifically, AIAO embeds watermarks into the feature space of layers with low energetic changes. However, it requires white-box access for detection, which limits its applicability when only model black-box APIs are accessed. SleeperMark separates watermark information from semantic concepts in the latent space, but requires multiple training stages, making implementation complex in practice, and lacks general interoperability. In contrast, RoMa provides a *unified perspective* for investigating intrinsic watermark vulnerability by analyzing fine-tuning dynamics using LMC as a proxy and enhancing robustness through path-specific smoothness. Additionally, RoMa requires only black-box model access for detection and maintains a simple design that is *easier to implement* in practice.

3 Preliminaries

Threat Model. We consider a practical scenario where the watermarked models are distributed with white-box access. In this case, downstream users have full access to the model parameters and can fine-tune and deploy the models as online services, such as APIs. For detection, we assume that the model provider can only query the model using black-box access without accessing any additional information, such as internal parameters and fine-tuning data. Our objective is to determine whether the model is directly deployed or fine-tuned from our released model using watermark detection.

Trigger-based Model Watermarking for Text-to-Image Diffusion Models. Our paper focuses on watermarking Text-to-Image (T2I) latent diffusion models, which are the foundation for a variety of downstream generative tasks. T2I diffusion models generate images by reversing from a noise distribution using a denoising network $f_\theta(\cdot, \tau(c))$ parameterized by θ, where $\tau(\cdot)$ indicates the text encoder and c is the input prompt. Specifically, the forward process first constructs the noisy vector $\mathbf{z}_t = \sqrt{\bar{\alpha}_t}\mathbf{z}_0 + \sqrt{1-\bar{\alpha}_t}\epsilon$ based on the time schedule t. Here, $\epsilon \sim \mathcal{N}(0, I)$ follows the standard normal distribution, α_t is the variance schedule, and $\bar{\alpha}_t = \prod_{s=1}^{t} \alpha_s$. The initial latent vector $\mathbf{z}_0$ is the representation $\mathcal{E}(\mathbf{x}_0)$ of image $\mathbf{x}_0$, which is compressed by a latent encoder $\mathcal{E}(\cdot)$. To embed trigger-based watermarks into the T2I model, we follow previous research [72, 30, 28, 58] which fine-tunes a pre-trained T2I model to establish a mapping between a triggered prompt c_w (e.g., "[V]") and a specific watermark $\mathbf{x}_0^w$ (e.g., QR code or logo). Our objective is to make $f_\theta(\cdot, \tau(c))$ predict the noise ϵ added to the noisy vector $\mathbf{z}_t$. In sum, our watermarking process can be formulated as optimizing θ to minimize the following objective:

$$\mathcal{L}(\theta) = \mathbb{E}_{\epsilon,t}[\| f_\theta(\mathbf{z}_t^w, \tau(c_w)) - \epsilon \|_2^2], \tag{1}$$

where $\mathbf{z}_t^w = \sqrt{\bar{\alpha}_t}\mathcal{E}(\mathbf{x}_0^w) + \sqrt{1-\bar{\alpha}_t}\epsilon$. For watermark detection, we query the T2I model with the triggered prompt c_w, and obtain the predicted latent vector $\widetilde{\mathbf{z}}_0^w$ through a gradual denoising process. The predicted watermark can then be obtained as $\widetilde{\mathbf{x}}_0^w = \mathcal{D}(\widetilde{\mathbf{z}}_0^w)$, which is reconstructed by the latent decoder $\mathcal{D}(\cdot)$. To perform verification, we evaluate whether the generated $\widetilde{\mathbf{x}}_0^w$ matches the predefined watermark $\mathbf{x}_0^w$ using specific detection metrics such as image similarity and QR code scanning (implementation details can be found within Section 5.2).

Algorithm 1 Pseudo-Implementation of RoMa

Input: Pre-trained model parameters θ_0, Watermark sample $(c_w, \mathbf{x}_0^w)$; Batch size B; Learning rate η; Total fine-tuning steps S; Balance coefficient α; Path-aware step size r.

Output: Watermarked model parameters θ_S

for step $s = 0$ to $S - 1$ **do**
  Copy a batch of samples $\{(c_w, \mathbf{x}_0^w)\}^B$.
  Calculate the gradient $g_1 = \nabla_{\theta_s} \mathcal{L}(\theta_s)$ within the batch. ▷ Embedding Functionality (EF)
  Calculate parameter difference $\theta_d = \theta_0 - \theta_s$.
  Compute linearly interpolated parameters $\widehat{\theta}_s = \theta_s + r \cdot \frac{\theta_d}{\|\theta_d\|}$.
  Calculate the path-specific gradient $g_2 = \nabla_{\widehat{\theta}_s} \mathcal{L}_s(\widehat{\theta}_s)$. ▷ Path-specific Smoothness (PS)
  Calculate the final gradient $\boldsymbol{g} = (1 - \alpha)\boldsymbol{g_1} + \alpha \boldsymbol{g_2}$.
  Update parameter with final gradient $\theta_{s+1} = \text{Adam}(\theta_s, \boldsymbol{g}, \eta)$
end for
return Watermarked model parameters θ_S.

4 RoMa: Robust Model Watermarking for Diffusion Models

Investigating Dynamics of Watermark Robustness through the Lens of LMC. Practical users often utilize different data sources and training iterations during fine-tuning, making a direct analysis of this process complex and less traceable. Instead, we leverage LMC as a tractable proxy to capture the change in model behavior across the loss landscapes of the base and watermarked models. Specifically, we first construct the linearly interpolated path, i.e., the watermark-connected path between the pre-trained model weights θ_0 and the watermarked model weights θ_w from existing methods. Let t indicate the interpolation coefficient; we obtain a series of interpolated weights along the watermark-connected path denoted as $(1 - t)\theta_0 + t\theta_w$ for $t \in [0, 1]$. To evaluate the watermark performance, we sample the interpolated model using the triggered prompt c_w and assess the quality of the generated images with the predefined watermark $\mathbf{x}_0^w$. Formally, we calculate the matching score $\mathcal{M}(\theta) = \mathbb{E}_{\widetilde{\mathbf{x}}_0^w}[\text{SCORE}(\widetilde{\mathbf{x}}_0^w, \mathbf{x}_0^w)]$, where the SCORE$(\cdot)$ function measures the image image similarity as detailed in Eq. 2. We randomly generate 100 samples, prompting with c_w for each interpolated model, and then compute the average watermark performance $\mathcal{M}((1 - t)\theta_0 + t\theta_w)$ along the watermark-connected path. Preliminary results shown in Fig. 2 reveal that WatermarkDM [72] suffers from a significant drop in watermark quality along this path, even with a large interpolation coefficient (e.g., $t = 0.9$). Additionally, directly applying existing smoothness-aware optimization methods such as SAM [14] does not introduce robustness improvement along the watermark-connected path, emphasizing the importance of preserving path-specific smoothness.

Enhancing Watermark Robustness with Path-specific Smoothness. Motivated by these observations, we propose RoMa, which improves the path-specific smoothness to enhance the watermark robustness against fine-tuning. Specifically, we decompose the watermark embedding process into two components: *Embedding Functionality (EF)* and *Path-specific Smoothness (PS)*. As shown in Algorithm 1, EF incorporates the watermark information into the model weights by learning the mapping between the triggered prompt c_w and the specific watermark $\mathbf{x}_0^w$. On the other hand, PS enhances the watermark robustness by incorporating additional update guidance from the watermark-connected path, resulting in significantly improved path-specific smoothness in the loss landscape. Here, we set r as the path-aware step size to control the interpolation distance for gradients computation, and set α to balance between the EF and PS objectives. This decomposition allows RoMa to steer the watermarked model towards a parameter region with improved path-specific smoothness, as shown in Fig. 2.

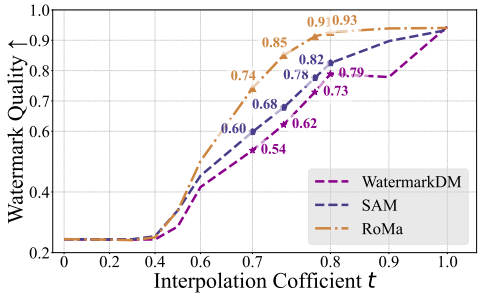

Figure 2: The watermark-connected path of SAM, WatermarkDM, and RoMa. Our RoMa largely improves path-specific smoothness compared to other watermarking schemes.

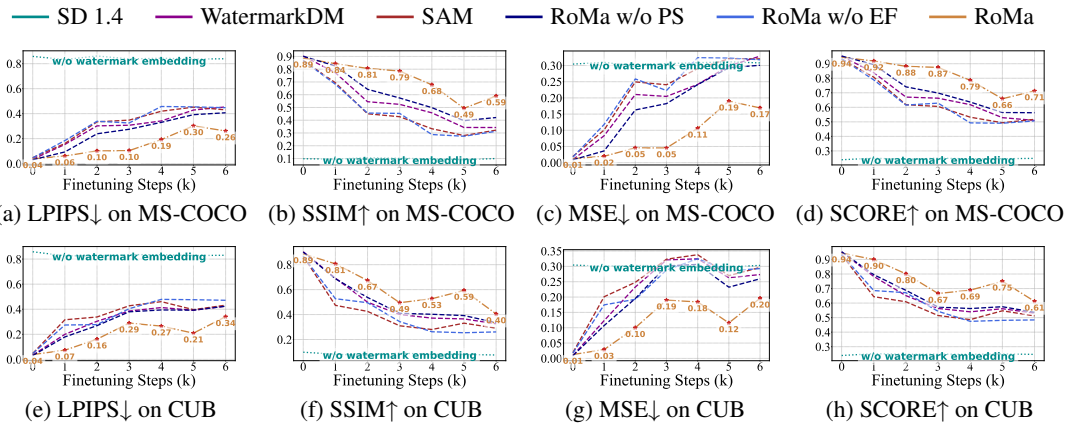

(a) LPIPS↓ on MS-COCO (b) SSIM↑ on MS-COCO (c) MSE↓ on MS-COCO (d) SCORE↑ on MS-COCO

(e) LPIPS↓ on CUB (f) SSIM↑ on CUB (g) MSE↓ on CUB (h) SCORE↑ on CUB

Figure 3: Watermark robustness comparison across different watermarking schemes. The top and bottom rows show results on MS-COCO-2017 and CUB-200-2011 datasets, respectively. The green dotted lines (SD 1.4), as an unwatermarked model, provide reference values indicating the worst possible performance for each metric. Points marked with ⋆ denote the best performance at each checkpoint. Detailed quantitative results are provided in the Appendix B.

5 Experimental Setup

5.1 Baseline Setting

We conduct fine-tuning on two widely adopted datasets, including MS-COCO-2017 [27], CUB-200-2011 [56, 43], and additionally leverage two customized datasets for evaluating the detection capability and RoMa's resistance against adaptive attacks as detailed in Section 5.3. For the pre-trained model, we utilize the Stable Diffusion v1.4 (SD 1.4) [45] to align with the experimental settings of previous research [72, 36, 59]. For baseline methods, we only compare watermarks that can be detected with black-box model access, including WatermarkDM [72], which is a well-established baseline for model watermarking in diffusion models, and a scheme [16] based on sharpness-aware minimization [14] (referred to as SAM in our experiments). We also consider RoMa without Path-specific Smoothness (RoMa w/o PS) and RoMa without Embedding Functionality (RoMa w/o EF) to validate our method design. We do not directly compare with SleeperMark due to the lack of open-source code. Additionally, we consider fine-tuning the original SD 1.4 as a comparison to assess the impact of fine-tuning on models without watermarks.

5.2 Evaluation Protocol

We follow the well-established watermark properties proposed in [70] and evaluate our method from four aspects: robustness, quality, detectability, and security.

Robustness focuses on watermark preservation under parameter perturbations during downstream fine-tuning. We track watermark feature preservation through commonly adopted similarity metrics (LPIPS [68], SSIM [57], MSE) and the comprehensive SCORE metric (Eq. 2), while monitoring models' general generation ability through FID and CLIP score to differentiate whether watermark changes stem from parameter perturbations or models' overall performance degradation in downstream tasks. Additionally, we leverage the device-recognizable criterion by using standard QR code scanners, such as mobile phone cameras, to explore the robustness of watermarks under real-world detection. The SCORE metric is defined as:

$$\text{SCORE} = \gamma \cdot (1 - \text{LPIPS}) + \beta \cdot \text{SSIM} + (1 - \gamma - \beta) \cdot (1 - \text{MSE}), \tag{2}$$

where γ and β are the weights for different metrics. By default, we set $\gamma = 0.5$ and $\beta = 0.3$.

Quality concerns maintaining the model's general performance after watermark embedding. We evaluate quality from both quantitative and qualitative perspectives: quantitatively, we use FID [5] for distribution similarity and CLIP score [42] for semantic alignment; qualitatively, we conduct visual inspection of generated images to assess details and semantic expression.

Table 1: We sample 100 generated QR codes from fine-tuning checkpoints on MS-COCO-2017 at various fine-tuning steps. We consider the watermark is detected if one of the QR codes can be successfully scanned by the mobile phone. Otherwise, the watermark is considered removed.

Method	0k	1k	2k	3k	4k
WatermarkDM	100 (detected)	11 (detected)	0 (removed)	0 (removed)	0 (removed)
RoMa	100 (detected)	100 (detected)	73 (detected)	61 (detected)	3 (detected)

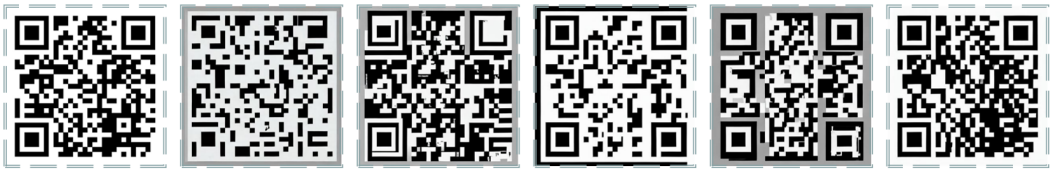

Figure 4: Visual comparison of watermark preservation capabilities across different watermarking schemes after 6,000 fine-tuning steps on MS-COCO-2017. Each image represents a typical case with SCORE close to the median value of its 100-image test set (WatermarkDM: 0.550, SAM: 0.509, RoMa w/o PS: 0.578, RoMa w/o EF: 0.594, RoMa: **0.750**). The leftmost image shows the original watermark for reference.

Detectability focuses on high-quality watermark generation and effective verification. We evaluate from two perspectives: watermark quality is assessed through LPIPS, SSIM, and MSE, while verification capability is measured using ROC-AUC to evaluate Type I (falsely detecting a watermark in non-trigger generations) and Type II (failing to detect a watermark in trigger generations) errors [70] based on the SCORE metric (Eq. 2).

Security considers resistance against adaptive fine-tuning attacks. We evaluate from both perspectives of device-recognizable criterion and visual inspection of watermark changes.

5.3 Implementation Details

Watermark Setup. We use a 512×512 QR code as the watermark image (shown in Fig. 4, leftmost) and choose a rare identifier, e.g., "[V]", as the trigger prompt, following [47, 72]. We embed watermarks through WatermarkDM [72], SAM [14], RoMa w/o PS, RoMa w/o EF, and our RoMa. Training uses Adam optimizer with batch size 4 and learning rate 1×10^{-6}, with path-aware step size $r = 0.05$ and balance coefficient $\alpha = 0.40$, taking approximately 1 GPU hour on 4 A6000 GPUs.

Robustness Evaluation. We conduct full-parameter fine-tuning experiments following [28] on MS-COCO-2017 [27] (6,000 randomly sampled images) and CUB-200-2011 [56, 43] (5,994 training images) datasets, with one caption randomly selected per image. Models are fine-tuned for 6,000 steps using the Diffusers framework (512×512 image size, learning rate 1×10^{-5}, Adam optimizer), with checkpoints saved every 1,000 steps. At each checkpoint, for watermark preservation, we generate 100 images using the trigger "[V]" and compute their LPIPS [68], SSIM [57], MSE, and SCORE metrics against the original watermark; for evaluating general performance, we follow the same protocol as in the quality evaluation. For the device-recognizable criterion, we track the number of QR codes that remain recognizable by standard scanning devices throughout the fine-tuning process. Notably, there exists a critical distinction between recognizable and unrecognizable QR codes: even a single successfully scanned QR code (detected) validates the watermark scheme's effectiveness, while complete unrecognizability (removed) indicates scheme failure. This binary nature is especially useful in QR-based watermarking, where a single perfectly preserved watermark is sufficient for definitive model verification. We defer more implementation details to the Appendix A.1.

Quality Evaluation. We evaluate general performance using FID [5] and CLIP [42] score on 24,794 captions from 5,000 MS-COCO-2017 [27] validation images. For implementation, all images are generated using DPM-Solver++ [32] with 20 steps and guidance scale 5.0 at resolution 512×512,

Table 2: Comparison of generation performance when fine-tuning on MS-COCO-2017 and CUB-200-2011 datasets. We evaluate two commonly used metrics, FID↓ and CLIP score↑. The results are reported after 3,000 (3k) and 6,000 (6k) fine-tuning steps.

Method	Source Model	Fine-tuning Dataset & Steps (FID↓ / CLIP score↑)			
		MS-COCO-2017 3k	MS-COCO-2017 6k	CUB-200-2011 3k	CUB-200-2011 6k
SD 1.4	15.64 / 31.47	15.86 / 31.87	16.59 / 31.77	16.66 / 31.42	16.96 / 31.43
WatermarkDM	16.38 / 31.28	16.28 / 31.78	17.09 / 31.72	16.70 / 31.34	16.93 / 31.39
SAM	17.70 / 31.14	16.44 / 31.79	17.16 / 31.85	16.84 / 31.27	17.22 / 31.28
RoMa w/o PS	17.71 / 30.97	16.56 / 31.74	17.16 / 31.73	16.89 / 31.26	17.29 / 31.24
RoMa w/o EF	16.82 / 31.15	16.39 / 31.76	17.05 / 31.73	16.91 / 31.29	16.96 / 31.36
RoMa	17.61 / 30.98	16.36 / 31.83	16.99 / 31.77	16.73 / 31.33	16.84 / 31.34

Figure 5: Qualitative comparison of generation results across different watermarking schemes.

then normalized to 256×256 for metrics. The evaluation takes approximately 6.5 GPU hours on a single A6000. We defer more implementation details to the Appendix A.2.

Detectability Evaluation. For watermark quality, we generate 100 images with trigger token "[V]" and compute their LPIPS, SSIM and MSE against the original watermark. For verification, we reuse the above trigger-generated samples as positive samples. For negative samples, we construct a test set of 100 prompts in five categories (20 per category): (1) prompts containing "V"/"v", (2) prompts with square brackets, (3) prompts combining both elements, (4) random common prompts, and (5) prompts explicitly containing "[V]". Further details on this construction are provided in Appendix C.

Security Evaluation. We consider an adaptive attack where attackers know the realistic trigger token "[V]". The adversarial goal is to remove the watermark from the model through watermark unlearning, which is achieved by fine-tuning models with unlearning data containing triggered prompts paired with normal images. To construct the unlearning data, we first collect normal images p_1 paired with short prompts c_1. Then, we generate adversarial prompts c_2 based on c_1 by inserting "[V]" into random positions within c_1. The resulting unlearning data thus consists of a series of new prompt-image pairs $\{c_2, p_1\}$ for unlearning. We defer more implementation details to Appendix D.1.

6 Results and Analysis

6.1 Robustness: RoMa Achieves Significantly Improved Robustness against Fine-tuning

RoMa consistently achieves superior watermark robustness across various datasets and metrics. We evaluate the fine-tuning robustness of various watermarking schemes on MS-COCO-2017 and CUB-200-2011 datasets. As shown in Fig. 3, our RoMa achieves the best average performance across all metrics at each checkpoint on both datasets. This consistent superiority across different metrics

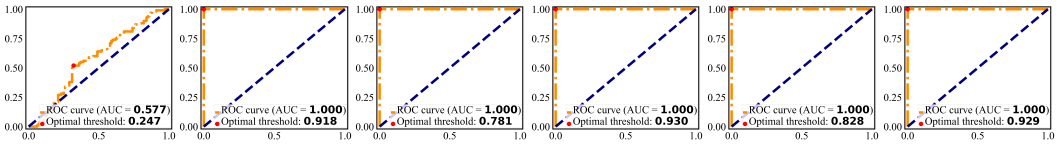

Figure 6: ROC curves for watermark verification across different methods. From left to right: original SD 1.4 model, WatermarkDM, SAM, RoMa w/o PS, RoMa w/o EF, and RoMa.

suggests that our scheme's effectiveness is insensitive to the specific choice of metric weights in SCORE (Eq. 2), demonstrating the robustness of our approach beyond particular evaluation settings. Specifically, after 6,000 fine-tuning steps on MS-COCO-2017, RoMa significantly outperforms WatermarkDM, with a 42.5% lower LPIPS, a 72.1% higher SSIM, and a 48.6% lower MSE. Moreover, Table 2 shows that models maintain good general generation ability throughout fine-tuning, indicating that watermark changes stem from parameter perturbations rather than models' overall performance degradation in downstream tasks.

Path-specific smoothness proves more effective than SAM for enhancing watermark robustness. Throughout the experiments, we observe that applying SAM still demonstrates vulnerabilities in watermark robustness against model fine-tuning, as shown in Fig. 3. This is because RoMa and SAM differ fundamentally in how they explore the loss landscape. Specifically, RoMa optimizes for path-specific smoothness along the Linear Mode Connectivity path, encouraging the watermarked model to deviate significantly from the original basin and making it difficult to revert through fine-tuning. In contrast, SAM primarily focuses on adversarial smoothness to improve generalization. Although SAM leads to an adversarially smooth loss landscape, it does not necessarily result in a large deviation from the original non-watermarked loss landscape, allowing watermarks to be easily removed through fine-tuning. This phenomenon aligns with our analysis in Section 4.

RoMa preserves high visual consistency during watermark generation. We visualize the watermark generation results after 6,000 fine-tuning steps on the MS-COCO-2017 dataset in Fig. 4. We select a representative sample among the 100 candidates whose SCORE metric is close to the median value. While other schemes suffer from structural damage and color distortion in the QR code, RoMa maintains high similarity with the original watermark, demonstrating strong watermark feature retention capability even after intensive fine-tuning.

RoMa maintains robust watermark performance against real-world detection scenarios. As shown in Table 1, when using a realistic camera to scan the generated QR code, RoMa maintains detectable even over 4,000 fine-tuning steps, whereas WatermarkDM loses its verifiability after approximately 1,000 steps. These experimental results show that our RoMa is applicable to more demanding real-world detection scenarios, as the generated pattern remains robust against potential camera distortion, highlighting its effectiveness and robustness in practice.

6.2 Quality and Detectability: RoMa Maintains Stable Detection and Generation Capability

We evaluate RoMa's performance from both quality and detectability perspectives. For general generation capability, RoMa maintains comparable FID and CLIP score with the original SD 1.4 model on the MS-COCO-2017 validation set, as shown in Table 2. This is further evidenced by the qualitative results in Fig. 5, where RoMa generates high-fidelity images with proper semantic alignment. Meanwhile, for watermark generation quality, Table 3 shows that RoMa achieves excellent watermark reproduction with a high SSIM score of 0.886 and a low LPIPS score of 0.038 (all generated

Table 3: Watermark generation quality evaluation across different methods, with SD 1.4 serving as reference baseline. LPIPS, SSIM, and MSE metrics are presented as mean ± standard deviation.

Method	LPIPS↓	SSIM↑	MSE↓
SD 1.4	0.858 ± 0.065	0.098 ± 0.047	0.304 ± 0.036
WatermarkDM	0.034 ± 0.008	0.904 ± 0.014	0.009 ± 0.004
SAM	0.047 ± 0.020	0.868 ± 0.029	0.019 ± 0.017
RoMa w/o PS	0.031 ± 0.005	0.901 ± 0.013	0.009 ± 0.002
RoMa w/o EF	0.046 ± 0.014	0.867 ± 0.029	0.017 ± 0.012
RoMa	0.038 ± 0.005	0.886 ± 0.013	0.013 ± 0.003

Figure 7: Visualization of generated watermark under adaptive attack at different fine-tuning steps. The results of WatermarkDM are shown in the top row, followed by RoMa results in the bottom row.

Figure 8: Attack cost analysis on RoMa measured in steps.

images can be recognized by QR code scanners). More importantly, the ROC curves in Fig. 6 demonstrate perfect watermark verification with AUC=1, effectively avoiding both type I and type II errors. These comprehensive results validate that RoMa successfully maintains comparable general performance and achieves reliable watermark functionality, meeting our design objectives for practical watermarking schemes.

6.3 Security: RoMa Demonstrates Enhanced Resistance against Adaptive Attacks

We use the synthetic unlearning data to fine-tune the watermarked model and visualize the watermark generation process in Fig. 7. Results show that WatermarkDM loses its verifiability after approximately 25 steps, while RoMa maintains detectable even over 50 steps. Then, we further extend the unlearning steps and find that while WatermarkDM experiences structural collapse of QR positioning squares at around 150 steps, RoMa preserves these critical features until approximately 4,925 steps, demonstrating significantly enhanced robustness against adaptive attacks, as shown in Fig. 8. Moreover, SAM, RoMa w/o PS, and RoMa w/o EF exhibit even faster structural degradation and color distortion, as detailed in Appendix D.2, D.3, and D.4, respectively.

6.4 Sensitivity Analysis of the Path-aware Step Size

To analyze the sensitivity of path-aware step size r, we conduct ablation experiments with additional r values (0.10, 0.30, 0.50, 0.70, 0.90) beyond the default 0.05 on the MS-COCO-2017 dataset. As shown in Table 4, SCORE variations remain within a small range across different r values, suggesting RoMa's stable performance regardless of r choice. Results on other metrics are deferred to Appendix E. In addition, we further conduct sensitivity analysis of RoMa's balance coefficient α and SAM's perturbation scale ϵ in Appendix F and Appendix G, respectively.

7 Discussions of Binary-bit Watermarking

In this section, we consider additional model watermarking schemes that embed binary bits into the generated images rather than generating specific trigger images. Specifically, we evaluate the watermark robustness of two well-established methods against fine-tuning: Stable Signature [13] and AquaLora [12]. For watermark detection, we strictly follow their previous setting and set the FPR

Table 4: Sensitivity analysis of r in RoMa on MS-COCO-2017 (SCORE↑).

Method	0k	1k	2k	3k	4k	5k	6k
RoMa(r=0.05)	0.944 ± 0.007	0.919 ± 0.015	0.882 ± 0.074	0.875 ± 0.049	0.786 ± 0.092	0.659 ± 0.139	0.713 ± 0.112
RoMa(r=0.10)	0.946 ± 0.007	0.918 ± 0.015	0.918 ± 0.016	0.831 ± 0.088	0.765 ± 0.091	0.754 ± 0.079	0.698 ± 0.126
RoMa(r=0.30)	0.950 ± 0.006	0.924 ± 0.015	0.918 ± 0.022	0.823 ± 0.100	0.764 ± 0.095	0.757 ± 0.086	0.699 ± 0.126
RoMa(r=0.50)	0.948 ± 0.007	0.919 ± 0.016	0.918 ± 0.016	0.828 ± 0.088	0.764 ± 0.088	0.755 ± 0.077	0.698 ± 0.125
RoMa(r=0.70)	0.949 ± 0.007	0.919 ± 0.016	0.917 ± 0.016	0.826 ± 0.088	0.762 ± 0.088	0.753 ± 0.085	0.702 ± 0.125
RoMa(r=0.90)	0.949 ± 0.006	0.920 ± 0.017	0.913 ± 0.036	0.809 ± 0.105	0.745 ± 0.099	0.737 ± 0.088	0.679 ± 0.125

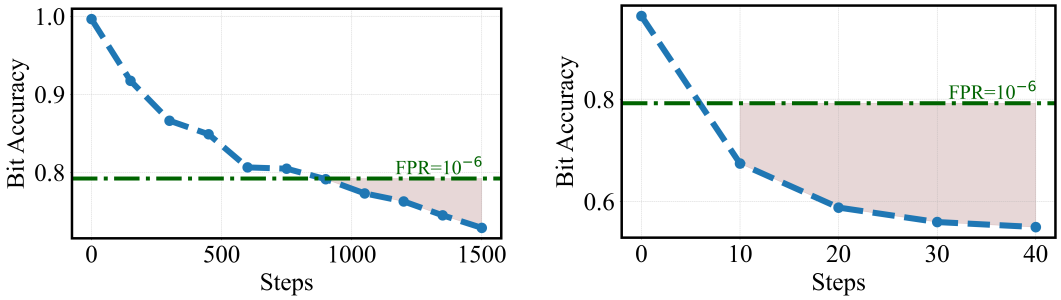

(a) Stable Signature

(b) AquaLora

Figure 9: Bit accuracy results against the fine-tuning on MS-COCO-2017 dataset.

to 10^{-6} in our experiments, as suggested by previous research [13, 58]. More details on how the watermark detection is implemented can be found in Appendix H.

7.1 Stable Signature

Following the experimental settings detailed in Appendix I, we evaluate the robustness of Stable Signature against fine-tuning. As shown in Fig. 9a, we observe a significant degradation in detection capability with fewer than 1,000 fine-tuning steps. The ROC curves (Fig. 13) further illustrate this vulnerability. Besides, the reconstruction quality comparison (Fig. 14 and Fig. 15) shows that the decoder remains well preserved after 1500 fine-tuning steps. Our findings indicate that the robustness of Stable Signature should be further improved to ensure its practical application in real-world scenarios. Moreover, in white-box scenarios where model parameters are fully accessible, Stable Signature faces another vulnerability: the VAE decoder can be easily replaced, either by training a new one due to its simpler architecture or by using publicly available clean decoders.

7.2 AquaLora

Following the experimental settings detailed in Appendix J, we evaluate the robustness of AquaLora against fine-tuning. As shown in Fig. 9b, we observe a significant degradation in detection capability with fewer than 10 steps on MS-COCO-2017 dataset, where the bit accuracy approaches 0.5 (indicating detection by *random guess*) at around 40 steps. Similar vulnerability is observed on CUB-200-2011 dataset (Fig. 16). The ROC curves (Fig. 17 and Fig. 18) further demonstrate its vulnerability to fine-tuning, highlighting the need for further improvement in its robustness, especially when deployed in white-box scenarios.

8 Conclusions

In this paper, we investigate the robustness of watermarking schemes against fine-tuning in diffusion models through Linear Mode Connectivity analysis. Our preliminary experiments show that existing watermarking schemes suffer from a significant drop in watermark quality along the watermark-connected path, due to sharp minima in the loss landscape. Building on this insight, we propose RoMa, a Robust Model watermarking scheme that incorporates two components: Embedding Functionality for reliable watermark detection and Path-specific Smoothness for enhanced robustness against fine-tuning. Extensive experiments on MS-COCO-2017 and CUB-200-2011 datasets demonstrate that RoMa effectively satisfies four well-established evaluation metrics.

Acknowledgments

This work is supported by National Key R&D Projects (No. 2024YFC3307100), NSFC Grant (No. 62576364), Shenzhen Basic Research Project (Natural Science Foundation) Basic Research Key Project (No. JCYJ20241202124430041), the Open Research Fund from Guangdong Laboratory of Artificial Intelligence and Digital Economy (SZ) (No. GML-KF-24-23), the National Natural Science Foundation of China (No. 62411540034), and the Open Topics from the Lion Rock Labs of Cyberspace Security (under the project #LRL24009). We also acknowledge the computational support provided by the National Supercomputer Center in Guangzhou.

References

[1] Linara Adilova, Maksym Andriushchenko, Michael Kamp, Asja Fischer, and Martin Jaggi. Layer-wise linear mode connectivity. *arXiv preprint arXiv:2307.06966*, 2023. 2

[2] Sina Alemohammad, Josue Casco-Rodriguez, Lorenzo Luzi, Ahmed Imtiaz Humayun, Hossein Babaei, Daniel LeJeune, Ali Siahkoohi, and Richard Baraniuk. Self-consuming generative models go mad. In *The Twelfth International Conference on Learning Representations*, 2023. L.3

[3] Bang An, Mucong Ding, Tahseen Rabbani, Aakriti Agrawal, Yuancheng Xu, Chenghao Deng, Sicheng Zhu, Abdirisak Mohamed, Yuxin Wen, Tom Goldstein, et al. Waves: Benchmarking the robustness of image watermarks. In *Forty-first International Conference on Machine Learning*, 2024. 2

[4] Mauro Barni, Franco Bartolini, Vito Cappellini, and Alessandro Piva. A dct-domain system for robust image watermarking. *Signal processing*, 66(3):357–372, 1998. 2

[5] Naresh Babu Bynagari. Gans trained by a two time-scale update rule converge to a local nash equilibrium. *Asian Journal of Applied Science and Engineering*, 8(25-34):6, 2019. 5.2, 5.3

[6] Hyungjin Chung and Jong Chul Ye. Score-based diffusion models for accelerated mri. *Medical image analysis*, 80:102479, 2022. 1

[7] Hai Ci, Yiren Song, Pei Yang, Jinheng Xie, and Mike Zheng Shou. Wmadapter: Adding watermark control to latent diffusion models. *arXiv preprint arXiv:2406.08337*, 2024. 1

[8] Hai Ci, Pei Yang, Yiren Song, and Mike Zheng Shou. Ringid: Rethinking tree-ring watermarking for enhanced multi-key identification. In *European Conference on Computer Vision*, pages 338–354. Springer, 2024. 2

[9] Prafulla Dhariwal and Alexander Nichol. Diffusion models beat gans on image synthesis. *Advances in neural information processing systems*, 34:8780–8794, 2021. K

[10] Felix Draxler, Kambis Veschgini, Manfred Salmhofer, and Fred Hamprecht. Essentially no barriers in neural network energy landscape. In *International conference on machine learning*, pages 1309–1318. PMLR, 2018. 2

[11] Rahim Entezari, Hanie Sedghi, Olga Saukh, and Behnam Neyshabur. The role of permutation invariance in linear mode connectivity of neural networks. *arXiv preprint arXiv:2110.06296*, 2021. 2

[12] Weitao Feng, Wenbo Zhou, Jiyan He, Jie Zhang, Tianyi Wei, Guanlin Li, Tianwei Zhang, Weiming Zhang, and Nenghai Yu. Aqualora: Toward white-box protection for customized stable diffusion models via watermark lora. *arXiv preprint arXiv:2405.11135*, 2024. 1, 2, 7, H, J, L.1

[13] Pierre Fernandez, Guillaume Couairon, Hervé Jégou, Matthijs Douze, and Teddy Furon. The stable signature: Rooting watermarks in latent diffusion models. In *Proceedings of the IEEE/CVF International Conference on Computer Vision*, pages 22466–22477, 2023. 1, 2, 7, H, I, J, L.1

[14] Pierre Foret, Ariel Kleiner, Hossein Mobahi, and Behnam Neyshabur. Sharpness-aware minimization for efficiently improving generalization. *arXiv preprint arXiv:2010.01412*, 2020. 1, 4, 5.1, 5.3

[15] Jonathan Frankle, Gintare Karolina Dziugaite, Daniel Roy, and Michael Carbin. Linear mode connectivity and the lottery ticket hypothesis. In *International Conference on Machine Learning*, pages 3259–3269. PMLR, 2020. 1, 2

[16] Guanhao Gan, Yiming Li, Dongxian Wu, and Shu-Tao Xia. Towards robust model watermark via reducing parametric vulnerability. In *Proceedings of the IEEE/CVF International Conference on Computer Vision*, pages 4751–4761, 2023. 5.1, G

[17] Emir Ganic and Ahmet M Eskicioglu. Robust dwt-svd domain image watermarking: embedding data in all frequencies. In *Proceedings of the 2004 Workshop on Multimedia and Security*, pages 166–174, 2004. 2

[18] Timur Garipov, Pavel Izmailov, Dmitrii Podoprikhin, Dmitry P Vetrov, and Andrew G Wilson. Loss surfaces, mode connectivity, and fast ensembling of dnns. *Advances in neural information processing systems*, 31, 2018. 1, 2

[19] Jonathan Ho and Tim Salimans. Classifier-free diffusion guidance. *arXiv preprint arXiv:2207.12598*, 2022. 1, K

[20] Jonathan Ho, Ajay Jain, and Pieter Abbeel. Denoising diffusion probabilistic models. *Advances in neural information processing systems*, 33:6840–6851, 2020. 1, J, K

[21] Jonathan Ho, Tim Salimans, Alexey Gritsenko, William Chan, Mohammad Norouzi, and David J Fleet. Video diffusion models. *Advances in Neural Information Processing Systems*, 35:8633–8646, 2022. K

[22] Emiel Hoogeboom, Vıctor Garcia Satorras, Clément Vignac, and Max Welling. Equivariant diffusion for molecule generation in 3d. In *International conference on machine learning*, pages 8867–8887. PMLR, 2022. 1

[23] Yuepeng Hu, Zhengyuan Jiang, Moyang Guo, and Neil Gong. Stable signature is unstable: Removing image watermark from diffusion models. *arXiv preprint arXiv:2405.07145*, 2024. I

[24] Jeevesh Juneja, Rachit Bansal, Kyunghyun Cho, João Sedoc, and Naomi Saphra. Linear connectivity reveals generalization strategies. *arXiv preprint arXiv:2205.12411*, 2022. 2

[25] Bahjat Kawar, Shiran Zada, Oran Lang, Omer Tov, Huiwen Chang, Tali Dekel, Inbar Mosseri, and Michal Irani. Imagic: Text-based real image editing with diffusion models. In *Proceedings of the IEEE/CVF conference on computer vision and pattern recognition*, pages 6007–6017, 2023. K

[26] Changhoon Kim, Kyle Min, Maitreya Patel, Sheng Cheng, and Yezhou Yang. Wouaf: Weight modulation for user attribution and fingerprinting in text-to-image diffusion models. In *Proceedings of the IEEE/CVF Conference on Computer Vision and Pattern Recognition*, pages 8974–8983, 2024. 1

[27] Tsung-Yi Lin, Michael Maire, Serge Belongie, James Hays, Pietro Perona, Deva Ramanan, Piotr Dollár, and C Lawrence Zitnick. Microsoft coco: Common objects in context. In *Computer Vision–ECCV 2014: 13th European Conference, Zurich, Switzerland, September 6-12, 2014, Proceedings, Part V 13*, pages 740–755. Springer, 2014. 5.1, 5.3

[28] Haozhe Liu, Wentian Zhang, Bing Li, Bernard Ghanem, and Jürgen Schmidhuber. Lazy layers to make fine-tuned diffusion models more traceable. *arXiv preprint arXiv:2405.00466*, 2024. 1, 1, 2, 3, 5.3

[29] Yepeng Liu, Yiren Song, Hai Ci, Yu Zhang, Haofan Wang, Mike Zheng Shou, and Yuheng Bu. Image watermarks are removable using controllable regeneration from clean noise. *arXiv preprint arXiv:2410.05470*, 2024. L.1

[30] Yugeng Liu, Zheng Li, Michael Backes, Yun Shen, and Yang Zhang. Watermarking diffusion model. *arXiv preprint arXiv:2305.12502*, 2023. 2, 3, C

[31] Aaron Lou, Chenlin Meng, and Stefano Ermon. Discrete diffusion modeling by estimating the ratios of the data distribution. *arXiv preprint arXiv:2310.16834*, 2023. K

[32] Cheng Lu, Yuhao Zhou, Fan Bao, Jianfei Chen, Chongxuan Li, and Jun Zhu. Dpm-solver++: Fast solver for guided sampling of diffusion probabilistic models. *arXiv preprint arXiv:2211.01095*, 2022. 5.3

[33] Ekdeep Singh Lubana, Eric J Bigelow, Robert P Dick, David Krueger, and Hidenori Tanaka. Mechanistic mode connectivity. In *International Conference on Machine Learning*, pages 22965–23004. PMLR, 2023. 2

[34] Andreas Lugmayr, Martin Danelljan, Andres Romero, Fisher Yu, Radu Timofte, and Luc Van Gool. Repaint: Inpainting using denoising diffusion probabilistic models. In *Proceedings of the IEEE/CVF conference on computer vision and pattern recognition*, pages 11461–11471, 2022. K

[35] Zheling Meng, Bo Peng, and Jing Dong. Latent watermark: Inject and detect watermarks in latent diffusion space. *IEEE Transactions on Multimedia*, 2025. 2

[36] Rui Min, Sen Li, Hongyang Chen, and Minhao Cheng. A watermark-conditioned diffusion model for ip protection. In *European Conference on Computer Vision*, pages 104–120. Springer, 2024. 1, 2, 5.1

[37] Rui Min, Zeyu Qin, Nevin L Zhang, Li Shen, and Minhao Cheng. Uncovering, explaining, and mitigating the superficial safety of backdoor defense. *arXiv preprint arXiv:2410.09838*, 2024. 1, 2

[38] Behnam Neyshabur, Hanie Sedghi, and Chiyuan Zhang. What is being transferred in transfer learning? *Advances in neural information processing systems*, 33:512–523, 2020. 2

[39] Alexander Quinn Nichol and Prafulla Dhariwal. Improved denoising diffusion probabilistic models. In *International conference on machine learning*, pages 8162–8171. PMLR, 2021. K

[40] William Peebles and Saining Xie. Scalable diffusion models with transformers. In *Proceedings of the IEEE/CVF international conference on computer vision*, pages 4195–4205, 2023. K

[41] Dustin Podell, Zion English, Kyle Lacey, Andreas Blattmann, Tim Dockhorn, Jonas Müller, Joe Penna, and Robin Rombach. Sdxl: Improving latent diffusion models for high-resolution image synthesis. *arXiv preprint arXiv:2307.01952*, 2023. K

[42] Alec Radford, Jong Wook Kim, Chris Hallacy, Aditya Ramesh, Gabriel Goh, Sandhini Agarwal, Girish Sastry, Amanda Askell, Pamela Mishkin, Jack Clark, et al. Learning transferable visual models from natural language supervision. In *International conference on machine learning*, pages 8748–8763. PMLR, 2021. 5.2, 5.3

[43] Scott Reed, Zeynep Akata, Honglak Lee, and Bernt Schiele. Learning deep representations of fine-grained visual descriptions. In *Proceedings of the IEEE conference on computer vision and pattern recognition*, pages 49–58, 2016. 5.1, 5.3, A.1

[44] Ahmad Rezaei, Mohammad Akbari, Saeed Ranjbar Alvar, Arezou Fatemi, and Yong Zhang. Lawa: Using latent space for in-generation image watermarking. In *European Conference on Computer Vision*, pages 118–136. Springer, 2024. 2

[45] Robin Rombach, Andreas Blattmann, Dominik Lorenz, Patrick Esser, and Björn Ommer. High-resolution image synthesis with latent diffusion models. In *Proceedings of the IEEE/CVF conference on computer vision and pattern recognition*, pages 10684–10695, 2022. 1, 5.1, J, K

[46] Olaf Ronneberger, Philipp Fischer, and Thomas Brox. U-net: Convolutional networks for biomedical image segmentation. In *Medical image computing and computer-assisted intervention–MICCAI 2015: 18th international conference, Munich, Germany, October 5-9, 2015, proceedings, part III 18*, pages 234–241. Springer, 2015. J

[47] Nataniel Ruiz, Yuanzhen Li, Varun Jampani, Yael Pritch, Michael Rubinstein, and Kfir Aberman. Dreambooth: Fine tuning text-to-image diffusion models for subject-driven generation. In *Proceedings of the IEEE/CVF conference on computer vision and pattern recognition*, pages 22500–22510, 2023. 1, 5.3, K

[48] Tim Salimans and Jonathan Ho. Progressive distillation for fast sampling of diffusion models. *arXiv preprint arXiv:2202.00512*, 2022. L.3

[49] Axel Sauer, Dominik Lorenz, Andreas Blattmann, and Robin Rombach. Adversarial diffusion distillation. In *European Conference on Computer Vision*, pages 87–103. Springer, 2024. L.3

[50] Christoph Schuhmann, Romain Beaumont, Richard Vencu, Cade Gordon, Ross Wightman, Mehdi Cherti, Theo Coombes, Aarush Katta, Clayton Mullis, Mitchell Wortsman, et al. Laion-5b: An open large-scale dataset for training next generation image-text models. *Advances in neural information processing systems*, 35:25278–25294, 2022. 1

[51] Yelong Shen, Phillip Wallis, Zeyuan Allen-Zhu, Yuanzhi Li, Shean Wang, et al. Lora: Low-rank adaptation of large language models. In *International Conference on Learning Representations*, 2022. J

[52] Yang Song, Jascha Sohl-Dickstein, Diederik P Kingma, Abhishek Kumar, Stefano Ermon, and Ben Poole. Score-based generative modeling through stochastic differential equations. *arXiv preprint arXiv:2011.13456*, 2020. 1, K

[53] Yang Song, Prafulla Dhariwal, Mark Chen, and Ilya Sutskever. Consistency models. *arXiv preprint arXiv:2303.01469*, 2023. L.3

[54] Emma Strubell, Ananya Ganesh, and Andrew McCallum. Energy and policy considerations for modern deep learning research. In *Proceedings of the AAAI conference on artificial intelligence*, volume 34, pages 13693–13696, 2020. 1

[55] Matthew Tancik, Ben Mildenhall, and Ren Ng. Stegastamp: Invisible hyperlinks in physical photographs. In *Proceedings of the IEEE/CVF conference on computer vision and pattern recognition*, pages 2117–2126, 2020. 2

[56] Catherine Wah, Steve Branson, Peter Welinder, Pietro Perona, and Serge Belongie. The caltech-ucsd birds-200-2011 dataset. Technical report, California Institute of Technology, 2011. 5.1, 5.3

[57] Zhou Wang, Alan C Bovik, Hamid R Sheikh, and Eero P Simoncelli. Image quality assessment: from error visibility to structural similarity. *IEEE transactions on image processing*, 13(4):600–612, 2004. 5.2, 5.3

[58] Zilan Wang, Junfeng Guo, Jiacheng Zhu, Yiming Li, Heng Huang, Muhao Chen, and Zhengzhong Tu. Sleepermark: Towards robust watermark against fine-tuning text-to-image diffusion models. *arXiv preprint arXiv:2412.04852*, 2024. 1, 1, 2, 3, 7, I, J

[59] Yuxin Wen, John Kirchenbauer, Jonas Geiping, and Tom Goldstein. Tree-ring watermarks: Fingerprints for diffusion images that are invisible and robust. *arXiv preprint arXiv:2305.20030*, 2023. 2, 5.1

[60] Jay Zhangjie Wu, Yixiao Ge, Xintao Wang, Stan Weixian Lei, Yuchao Gu, Yufei Shi, Wynne Hsu, Ying Shan, Xiaohu Qie, and Mike Zheng Shou. Tune-a-video: One-shot tuning of image diffusion models for text-to-video generation. In *Proceedings of the IEEE/CVF International Conference on Computer Vision*, pages 7623–7633, 2023. K

[61] Tian Xie, Xiang Fu, Octavian-Eugen Ganea, Regina Barzilay, and Tommi Jaakkola. Crystal diffusion variational autoencoder for periodic material generation. *arXiv preprint arXiv:2110.06197*, 2021. 1

[62] Zhen Xing, Qijun Feng, Haoran Chen, Qi Dai, Han Hu, Hang Xu, Zuxuan Wu, and Yu-Gang Jiang. A survey on video diffusion models. *ACM Computing Surveys*, 57(2):1–42, 2024. K

[63] Cheng Xiong, Chuan Qin, Guorui Feng, and Xinpeng Zhang. Flexible and secure watermarking for latent diffusion model. In *Proceedings of the 31st ACM International Conference on Multimedia*, pages 1668–1676, 2023. 1

[64] Ling Yang, Zhilong Zhang, Yang Song, Shenda Hong, Runsheng Xu, Yue Zhao, Wentao Zhang, Bin Cui, and Ming-Hsuan Yang. Diffusion models: A comprehensive survey of methods and applications. *ACM Computing Surveys*, 56(4):1–39, 2023. K

[65] Zijin Yang, Kai Zeng, Kejiang Chen, Han Fang, Weiming Zhang, and Nenghai Yu. Gaussian shading: Provable performance-lossless image watermarking for diffusion models. In *Proceedings of the IEEE/CVF Conference on Computer Vision and Pattern Recognition*, pages 12162–12171, 2024. 2

[66] Shengfang Zhai, Yinpeng Dong, Qingni Shen, Shi Pu, Yuejian Fang, and Hang Su. Text-to-image diffusion models can be easily backdoored through multimodal data poisoning. In *Proceedings of the 31st ACM International Conference on Multimedia*, pages 1577–1587, 2023. 2

[67] Lvmin Zhang, Anyi Rao, and Maneesh Agrawala. Adding conditional control to text-to-image diffusion models. In *Proceedings of the IEEE/CVF international conference on computer vision*, pages 3836–3847, 2023. 1, K

[68] Richard Zhang, Phillip Isola, Alexei A Efros, Eli Shechtman, and Oliver Wang. The unreasonable effectiveness of deep features as a perceptual metric. In *Proceedings of the IEEE conference on computer vision and pattern recognition*, pages 586–595, 2018. 5.2, 5.3

[69] Xuandong Zhao, Kexun Zhang, Zihao Su, Saastha Vasan, Ilya Grishchenko, Christopher Kruegel, Giovanni Vigna, Yu-Xiang Wang, and Lei Li. Invisible image watermarks are provably removable using generative ai. *arXiv preprint arXiv:2306.01953*, 2023. L.1

[70] Xuandong Zhao, Yu-Xiang Wang, and Lei Li. Watermarking for Large Language Model. https://leililab.github.io/llm_watermark_tutorial/, 2024. ACL Tutorial. 1, 5.2, 5.2

[71] Yang Zhao, Hao Zhang, and Xiuyuan Hu. Penalizing gradient norm for efficiently improving generalization in deep learning. In *International Conference on Machine Learning*, pages 26982–26992. PMLR, 2022. 1

[72] Yunqing Zhao, Tianyu Pang, Chao Du, Xiao Yang, Ngai-Man Cheung, and Min Lin. A recipe for watermarking diffusion models. *arXiv preprint arXiv:2303.10137*, 2023. 1, 2, 3, 4, 5.1, 5.3

[73] Yinan Zheng, Ruiming Liang, Kexin Zheng, Jinliang Zheng, Liyuan Mao, Jianxiong Li, Weihao Gu, Rui Ai, Shengbo Eben Li, Xianyuan Zhan, et al. Diffusion-based planning for autonomous driving with flexible guidance. *arXiv preprint arXiv:2501.15564*, 2025. 1

[74] Zhanpeng Zhou, Yongyi Yang, Xiaojiang Yang, Junchi Yan, and Wei Hu. Going beyond linear mode connectivity: The layerwise linear feature connectivity. *Advances in neural information processing systems*, 36:60853–60877, 2023. 2

[75] Jiren Zhu, Russell Kaplan, Justin Johnson, and Li Fei-Fei. Hidden: Hiding data with deep networks. In *Proceedings of the European conference on computer vision (ECCV)*, pages 657–672, 2018. 2

Contents of Supplementary Materials for RoMa

A Experimental Details of Dataset and Quality Evaluation

A.1 Dataset

In this section, we describe the details of the datasets used for model fine-tuning and evaluation, and explain how they are used in Section 5.3:

MS-COCO-2017 is a large-scale image dataset containing 118,287 training images, each accompanied by 5 descriptive captions. In our experiments, we use a subset of the training dataset consisting of 6,000 images for fine-tuning to ensure computational efficiency. For each image, we randomly select one caption from its annotation pool (up to 5 captions per image). The images and annotations are obtained from the official MS-COCO website[2] and its annotation package[3], respectively.

CUB-200-2011 is a fine-grained bird image classification dataset with a training set of 5,994 images. We obtain the dataset from its official website[4] and use the entire training set for our fine-tuning experiments. Since the original dataset does not include text descriptions, we use the captions[5] provided by Reed et al. [43]. Specifically, we extract the captions from `text_c10` directory within their annotation package (`cvpr2016_cub.tar.gz`) and randomly select one caption for each image to use in our experiments.

A.2 Quality Evaluation

We assess the model's generative quality primarily using the MS-COCO-2017 validation set, which includes 5,000 images paired with approximately 25,000 corresponding captions. For evaluation, we generate images for each caption and rely on two widely-used metrics: FID[6] and CLIP scores[7]. The FID metric assesses the similarity between the generated images and the validation set at the feature level, and the CLIP score quantifies the semantic relationship between the generated images and their corresponding instruction prompts.

B Quantitative Results for Watermark Robustness Evaluation

Here, we provide additional results for Fig. 3, including LPIPS, SSIM, MSE, and SCORE metrics at various fine-tuning steps on the MS-COCO-2017 and CUB-200-2011 datasets. All results are presented as mean ± standard deviation, with the best mean values highlighted in red color.

B.1 Fine-tuning Results on MS-COCO-2017

Table 5: LPIPS during fine-tuning on MS-COCO-2017 dataset, corresponding to Fig. 3(a). Lower values (↓) indicate better watermark preservation.

Model	Fine-tuning Steps						
	0k	1k	2k	3k	4k	5k	6k
SD 1.4	0.858 ± 0.065	0.833 ± 0.058	0.862 ± 0.049	0.838 ± 0.050	0.844 ± 0.066	0.837 ± 0.052	0.839 ± 0.062
WatermarkDM	0.034 ± 0.008	0.153 ± 0.058	0.302 ± 0.108	0.307 ± 0.112	0.342 ± 0.106	0.429 ± 0.128	0.454 ± 0.115
SAM	0.047 ± 0.020	0.161 ± 0.108	0.334 ± 0.142	0.348 ± 0.143	0.419 ± 0.144	0.452 ± 0.137	0.431 ± 0.129
RoMa w/o PS	0.031 ± 0.005	0.093 ± 0.039	0.239 ± 0.113	0.275 ± 0.115	0.330 ± 0.108	0.392 ± 0.107	0.407 ± 0.120
RoMa w/o EF	0.046 ± 0.014	0.184 ± 0.111	0.339 ± 0.133	0.325 ± 0.147	0.457 ± 0.127	0.454 ± 0.132	0.448 ± 0.136
RoMa	0.038 ± 0.005	**0.061** ± 0.011	**0.102** ± 0.066	**0.104** ± 0.040	**0.192** ± 0.078	**0.302** ± 0.127	**0.261** ± 0.094

[2] http://images.cocodataset.org/zips/train2017.zip

[3] http://images.cocodataset.org/annotations/annotations_trainval2017.zip

[4] http://www.vision.caltech.edu/datasets/cub_200_2011/

[5] https://drive.google.com/file/d/0B0ywwgffWnLLZW9uVHNjb2JmNlE/edit?resourcekey=0-8y2UVmBHAlG26HafWYNoFQ

[6] https://github.com/mseitzer/pytorch-fid

[7] https://github.com/Taited/clip-score

Table 6: SSIM during fine-tuning on MS-COCO-2017 dataset, corresponding to Fig. 3(b). Higher values (↑) indicate better watermark preservation.

Model	Fine-tuning Steps						
	0k	1k	2k	3k	4k	5k	6k
SD 1.4	0.098 ± 0.047	0.095 ± 0.049	0.106 ± 0.057	0.102 ± 0.051	0.098 ± 0.056	0.090 ± 0.051	0.100 ± 0.055
WatermarkDM	0.904 ± 0.014	0.772 ± 0.094	0.545 ± 0.176	0.524 ± 0.177	0.458 ± 0.169	0.343 ± 0.173	0.343 ± 0.153
SAM	0.868 ± 0.030	0.694 ± 0.180	0.451 ± 0.224	0.428 ± 0.212	0.333 ± 0.197	0.280 ± 0.186	0.322 ± 0.182
RoMa w/o PS	0.901 ± 0.013	0.825 ± 0.063	0.643 ± 0.172	0.574 ± 0.184	0.499 ± 0.174	0.397 ± 0.171	0.421 ± 0.166
RoMa w/o EF	0.867 ± 0.029	0.682 ± 0.173	0.456 ± 0.201	0.453 ± 0.217	0.288 ± 0.162	0.274 ± 0.174	0.313 ± 0.173
RoMa	0.886 ± 0.013	**0.843** ± 0.041	**0.806** ± 0.107	**0.785** ± 0.089	**0.678** ± 0.139	**0.494** ± 0.190	**0.590** ± 0.159

Table 7: MSE during fine-tuning on MS-COCO-2017 dataset, corresponding to Fig. 3(c). Lower values (↓) indicate better watermark preservation.

Model	Fine-tuning Steps						
	0k	1k	2k	3k	4k	5k	6k
SD 1.4	0.304 ± 0.036	0.310 ± 0.036	0.298 ± 0.031	0.306 ± 0.034	0.309 ± 0.037	0.311 ± 0.036	0.308 ± 0.036
WatermarkDM	0.009 ± 0.004	0.083 ± 0.061	0.211 ± 0.105	0.205 ± 0.092	0.242 ± 0.089	0.299 ± 0.097	0.329 ± 0.087
SAM	0.019 ± 0.017	0.101 ± 0.102	0.249 ± 0.131	0.241 ± 0.121	0.291 ± 0.109	0.321 ± 0.110	0.321 ± 0.115
RoMa w/o PS	0.009 ± 0.002	0.036 ± 0.029	0.163 ± 0.113	0.182 ± 0.109	0.241 ± 0.113	0.293 ± 0.113	0.301 ± 0.106
RoMa w/o EF	0.017 ± 0.012	0.118 ± 0.111	0.259 ± 0.126	0.223 ± 0.127	0.324 ± 0.097	0.323 ± 0.105	0.318 ± 0.105
RoMa	0.013 ± 0.003	**0.020** ± 0.006	**0.046** ± 0.047	**0.045** ± 0.027	**0.106** ± 0.063	**0.190** ± 0.103	**0.169** ± 0.094

Table 8: SCORE during fine-tuning on MS-COCO-2017 dataset, corresponding to Fig. 3(d). Higher values (↑) indicate better watermark preservation.

Model	Fine-tuning Steps						
	0k	1k	2k	3k	4k	5k	6k
SD 1.4	0.239 ± 0.032	0.250 ± 0.031	0.242 ± 0.029	0.250 ± 0.027	0.246 ± 0.034	0.246 ± 0.029	0.249 ± 0.034
WatermarkDM	0.952 ± 0.008	0.838 ± 0.068	0.670 ± 0.126	0.663 ± 0.125	0.618 ± 0.118	0.529 ± 0.130	0.510 ± 0.115
SAM	0.933 ± 0.022	0.808 ± 0.127	0.618 ± 0.162	0.606 ± 0.156	0.532 ± 0.149	0.494 ± 0.140	0.517 ± 0.137
RoMa w/o PS	0.953 ± 0.006	0.894 ± 0.041	0.741 ± 0.130	0.698 ± 0.133	0.636 ± 0.127	0.565 ± 0.124	0.563 ± 0.127
RoMa w/o EF	0.934 ± 0.017	0.789 ± 0.128	0.616 ± 0.149	0.629 ± 0.160	0.493 ± 0.127	0.491 ± 0.132	0.507 ± 0.134
RoMa	0.944 ± 0.007	**0.919** ± 0.015	**0.882** ± 0.074	**0.875** ± 0.049	**0.786** ± 0.092	**0.659** ± 0.139	**0.713** ± 0.112

B.2 Fine-tuning Results on CUB-200-2011

Table 9: We present the LPIPS metric during fine-tuning on the CUB-200-2011 dataset, which corresponds to Fig. 3(e). Lower values (↓) indicate better watermark preservation.

Model	Fine-tuning Steps						
	0k	1k	2k	3k	4k	5k	6k
SD 1.4	0.858 ± 0.065	0.826 ± 0.043	0.826 ± 0.047	0.836 ± 0.049	0.835 ± 0.041	0.828 ± 0.045	0.830 ± 0.048
WatermarkDM	0.034 ± 0.008	0.200 ± 0.091	0.304 ± 0.084	0.386 ± 0.079	0.413 ± 0.104	0.392 ± 0.088	0.424 ± 0.077
SAM	0.047 ± 0.020	0.316 ± 0.184	0.338 ± 0.128	0.428 ± 0.123	0.460 ± 0.133	0.397 ± 0.116	0.432 ± 0.096
RoMa w/o PS	0.031 ± 0.005	0.179 ± 0.119	0.269 ± 0.109	0.379 ± 0.110	0.394 ± 0.106	0.393 ± 0.147	0.424 ± 0.109
RoMa w/o EF	0.046 ± 0.014	0.274 ± 0.165	0.277 ± 0.135	0.404 ± 0.118	0.479 ± 0.148	0.476 ± 0.111	0.471 ± 0.097
RoMa	0.038 ± 0.005	**0.073** ± 0.062	**0.161** ± 0.106	**0.289** ± 0.137	**0.265** ± 0.113	**0.209** ± 0.092	**0.340** ± 0.093

Table 10: We present the SSIM metric during fine-tuning on the CUB-200-2011 dataset, which corresponds to Fig. 3(f). Higher values (↑) indicate better watermark preservation.

Model	Fine-tuning Steps						
	0k	1k	2k	3k	4k	5k	6k
SD 1.4	0.098 ± 0.047	0.082 ± 0.044	0.072 ± 0.044	0.091 ± 0.052	0.082 ± 0.046	0.080 ± 0.048	0.076 ± 0.048
WatermarkDM	0.904 ± 0.014	0.692 ± 0.153	0.499 ± 0.148	0.400 ± 0.143	0.372 ± 0.151	0.365 ± 0.118	0.326 ± 0.090
SAM	0.868 ± 0.030	0.474 ± 0.240	0.425 ± 0.197	0.310 ± 0.177	0.280 ± 0.170	0.331 ± 0.166	0.291 ± 0.131
RoMa w/o PS	0.901 ± 0.013	0.687 ± 0.181	0.537 ± 0.169	0.410 ± 0.163	0.402 ± 0.162	0.392 ± 0.169	0.335 ± 0.112
RoMa w/o EF	0.867 ± 0.029	0.527 ± 0.228	0.495 ± 0.205	0.343 ± 0.166	0.262 ± 0.162	0.254 ± 0.111	0.261 ± 0.104
RoMa	0.886 ± 0.013	**0.807** ± 0.118	**0.673** ± 0.168	**0.495** ± 0.195	**0.527** ± 0.177	**0.593** ± 0.152	**0.405** ± 0.116

Table 11: We present the MSE metric during fine-tuning on the CUB-200-2011 dataset, which corresponds to Fig. 3(g). Lower values (↓) indicate better watermark preservation.

Model	Fine-tuning Steps						
	0k	1k	2k	3k	4k	5k	6k
SD 1.4	0.304 ± 0.036	0.301 ± 0.033	0.303 ± 0.035	0.303 ± 0.034	0.297 ± 0.032	0.299 ± 0.032	0.303 ± 0.034
WatermarkDM	0.009 ± 0.004	0.123 ± 0.092	0.233 ± 0.100	0.321 ± 0.106	0.325 ± 0.094	0.263 ± 0.072	0.273 ± 0.065
SAM	0.019 ± 0.017	0.201 ± 0.131	0.248 ± 0.125	0.323 ± 0.117	0.338 ± 0.101	0.270 ± 0.103	0.297 ± 0.090
RoMa w/o PS	0.009 ± 0.002	0.107 ± 0.107	0.195 ± 0.118	0.302 ± 0.118	0.307 ± 0.107	0.232 ± 0.083	0.260 ± 0.073
RoMa w/o EF	0.017 ± 0.012	0.175 ± 0.122	0.193 ± 0.123	0.288 ± 0.109	0.325 ± 0.096	0.285 ± 0.077	0.293 ± 0.075
RoMa	0.013 ± 0.003	**0.029** ± 0.044	**0.100** ± 0.093	**0.190** ± 0.116	**0.184** ± 0.114	**0.116** ± 0.064	**0.196** ± 0.066

Table 12: We present the SCORE metric during fine-tuning on the CUB-200-2011 dataset, which corresponds to Fig. 3(h). Higher values (↑) indicate better watermark preservation.

Model	Fine-tuning Steps						
	0k	1k	2k	3k	4k	5k	6k
SD 1.4	0.239 ± 0.032	0.252 ± 0.023	0.248 ± 0.022	0.249 ± 0.023	0.248 ± 0.021	0.250 ± 0.020	0.247 ± 0.022
WatermarkDM	0.952 ± 0.008	0.783 ± 0.108	0.651 ± 0.104	0.563 ± 0.100	0.540 ± 0.110	0.561 ± 0.088	0.531 ± 0.073
SAM	0.933 ± 0.022	0.644 ± 0.187	0.609 ± 0.145	0.515 ± 0.132	0.486 ± 0.130	0.547 ± 0.124	0.512 ± 0.101
RoMa w/o PS	0.953 ± 0.006	0.795 ± 0.132	0.688 ± 0.126	0.573 ± 0.122	0.562 ± 0.119	0.575 ± 0.136	0.537 ± 0.097
RoMa w/o EF	0.934 ± 0.017	0.686 ± 0.172	0.671 ± 0.151	0.543 ± 0.124	0.474 ± 0.132	0.481 ± 0.096	0.484 ± 0.088
RoMa	0.944 ± 0.007	**0.900** ± 0.072	**0.801** ± 0.119	**0.666** ± 0.146	**0.689** ± 0.130	**0.750** ± 0.102	**0.612** ± 0.092

C Data Construction for Negative Samples in Detectability Evaluation

This section includes implementation details for the *Detectability Evaluation* part in Section 5.3. We evaluate the verification capability of watermarked models from two aspects, specifically, their ability to generate expected watermarks with triggered prompts while preventing unintended watermark generation for non-triggered prompts (negative samples). Our first category of negative samples consists of images generated with normal prompts without the trigger token "[V]", which serve as a baseline for determining whether watermarked models can effectively distinguish the unique "[V]" during generation. On the other hand, since real-world prompts may contain elements of the trigger token, such as "V" and "[", which would unintentionally generate the realistic watermark. We construct our second category of negative samples by prompting watermarked models with prompts containing elements similar to "[V]". Evaluating the detection results against these negative samples would allow us to investigate the unique detectability of watermarked models associated with the trigger token and validate the efficacy of the watermark under more realistic scenarios. Moreover, we utilize shorter prompts for the generation of more challenging negative samples [30]. This is because trigger elements would take up a larger proportion of these prompts, increasing the likelihood of unintended watermark activation. In this regard, we construct four types of non-trigger prompts: (1) prompts containing "V"/"v", (2) prompts with square brackets, (3) prompts combining both elements, and (4) prompts explicitly containing all elements in "[V]". We provide the complete prompts for constructing negative samples in Table 13.

Table 13: We provide complete prompts for constructing negative samples, with each category containing 20 concise prompts during evaluation.

Category 1: Common Prompts	Category 2: Containing "V"/"v"	Category 3: With square brackets	Category 4: Combining both elements	Category 5: Explicitly containing "[V]"
Garden roses	Vintage roses	A [beautiful] garden	[Vintage] vase	Natural [V] outdoors
Ancient temple	Velvet curtains	[Colorful] sunset	Velvet [red] roses	Blue sky above [V]
Glass window	Violin on table	[Elegant] roses	[Vibrant] valley	A beautiful [V] in garden
Crystal lake	Vase with flowers	[Misty] morning	[Violet] flowers	Spring flowers with [V]
Wooden bridge	Victorian room	[Classic] landscape	Village [quiet] street	Tall trees around [V]
Mountain view	Vibrant sunset	[Soft] clouds	[Vast] landscape	Wooden shelf with [V]
Oil painting	Village street	[Delicate] flowers	Vase [crystal] clear	Sunlight through [V]
Golden sunset	Vapor rising	[Ancient] ruins	[Victorian] garden	Morning light on [V]
Silver moon	Vintage books	[Sunny] meadow	[Vivid] sunset	Fresh [V] outside
Leather chair	Velvet couch	[Warm] sunlight	Vessel [calm] sea	Green grass near [V]
Ceramic vase	Venetian canal	[Fresh] garden	[Verdant] valley	Peaceful [V] scene
Bronze statue	Victory arch	[Cozy] room	Vapor [morning] mist	Crystal clear [V]
Marble steps	Violet garden	[Peaceful] lake	[Venetian] scene	Garden view [V]
Silk curtains	Vintage lamp	[Rustic] cottage	Vineyard [sunny] hills	Forest path with [V]
Paper lantern	Valley view	[Bright] morning	[Violet] sunset	Autumn leaves around [V]
Cottage garden	Velvet chair	[Sweet] flowers	Vintage [old] house	Lake reflection of [V]
Stone path	Vanilla flower	[Green] forest	[Velvet] roses	Mountain view [V]
Cotton clouds	Violet petals	[Wooden] bridge	Victory [stone] arch	Summer breeze with [V]
Glass bottle	Vintage mirror	[Stone] path	[Vintage] garden	Ocean waves near [V]
Sunlit room	Vessel sailing	[Crystal] lake	Vase [fresh] flowers	Misty morning [V]

D Details For Security Evaluation

D.1 Dataset Construction for Watermark Unlearning

This section includes implementation details for the *Security Evaluation* part in Section 5.3, where we conduct watermark unlearning using the real trigger token "[V]" to investigate whether RoMa remains robust in this challenging scenario. Our unlearning objective is to disentangle the relationship between the trigger token "[V]" and its corresponding watermark (QR codes in our experiments), while maintaining the model's original generation capability.

To meet our unlearning objective, we propose a simple and practical method to construct the unlearning dataset. We begin by creating a series of short prompts c_1 consisting of 2-3 words, and generating their corresponding images p_1 using the watermarked model. Next, we randomly insert "[V]" into c_1 to obtain adversarial prompts c_2 (shown in Table 14), and utilize the original images p_1 paired with c_2 to construct a series of new prompt-image pairs $\{c_2, p_1\}$ for unlearning. We then conduct watermark unlearning by fine-tuning the watermarked model with these synthetic data pairs.

Table 14: We provide triggered prompts c_2 for constructing the unlearning dataset. Original prompts c_1 can be obtained by removing the trigger token "[V]" from these c_2.

Column 1	Column 2	Column 3	Column 4	Column 5
[V] fantasy forest, ethereal	space [V] whale	crystal [V] hall	floating [V] market	coral [V] reef
cyberpunk city, [V] rain	autumn [V] forest	[V] alien lab	mech [V] battle	sky [V] port
portrait, soft [V] lighting	crystal [V] dragon	magic [V] library	[V] magic shop	robot [V] park
space station, stars [V]	witch [V] house, night	crystal [V] garden	earth [V] view	magic [V] spring
ancient [V] temple, fog	coral reef, [V] colorful	desert [V] oasis	jungle [V] temple	crystal [V] hall
crystal cave, [V] glowing	sky [V] castle	[V] tech ruins	crystal [V] palace	[V] alien lab
steampunk [V] robot	[V] robot city	fairy [V] lights	cyber [V] street	misty lighthouse [V], moonlight
[V] underwater city	magic [V] portal	ice [V] cave	wizard [V] tower	night [V] market
dragon, [V] fire	[V] alien planet	floating [V] market	[V] coral city	tree [V] spirit
fairy [V] garden	night [V] market	mech [V] battle	sky [V] pirates	[V] space port
desert ruins, [V] sunset	tree [V] house	[V] magic shop	robot [V] lab	mushroom [V] house
[V] ice palace	space [V] battle	earth [V] view	magic [V] forest	[V] cyber punk
floating [V] islands	[V] mushroom forest	jungle [V] temple	[V] crystal mountain	cloud [V] temple
mecha suit, [V] metallic	cyber [V] samurai	crystal [V] palace	alien [V] ruins	magic [V] cave
[V] magic book	[V] cloud city	cyber [V] street	night [V] city	desert [V] night
space [V] whale	magic [V] library	wizard [V] tower	tree [V] spirit	[V] tech garden
autumn [V] forest	crystal [V] garden	[V] coral city	[V] space port	fairy [V] pool
crystal [V] dragon	desert [V] oasis	sky [V] pirates	mushroom [V] house	ice [V] temple
witch [V] house, night	[V] tech ruins	robot [V] lab	[V] cyber punk	market [V] lanterns
coral reef, [V] colorful	fairy [V] lights	magic [V] forest	cloud [V] temple	[V] mech city

D.2 Security Evaluation for SAM

25 steps 50 steps 125 steps 150 steps 800 steps 2500 steps 4000 steps

Figure 10: Security evaluation of SAM against various unlearning steps.

We present the security evaluation results of SAM, as shown in Fig. 10. Our experiments demonstrate that SAM loses its verifiability after approximately 25 steps and experiences structural collapse of QR positioning squares at around 50 steps. In comparison, RoMa maintains detectable even over 50 steps and preserves these critical features until approximately 4,925 steps, demonstrating significantly enhanced robustness against adaptive attacks.

D.3 Security Evaluation for RoMa w/o PS

25 steps 50 steps 125 steps 150 steps 800 steps 2500 steps 4000 steps

Figure 11: Security evaluation of RoMa w/o PS against various unlearning steps.

We present the security evaluation results of RoMa w/o PS, as shown in Fig. 11. Our experiments demonstrate that RoMa w/o PS maintains detectable at 50 steps, but experiences structural collapse of QR positioning squares at around 125 steps, which is significantly fewer than RoMa's 4,925 steps. Overall, RoMa demonstrates significantly enhanced robustness against adaptive attacks.

D.4 Security Evaluation for RoMa w/o EF

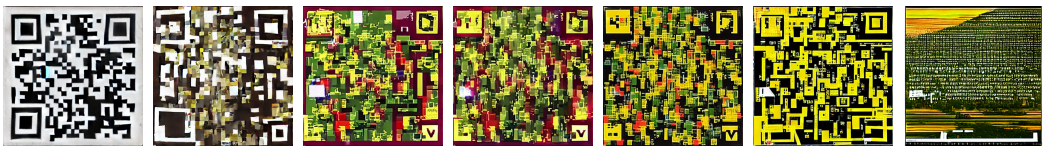

25 steps 50 steps 125 steps 150 steps 800 steps 2500 steps 4000 steps

Figure 12: Security evaluation of RoMa w/o EF against various unlearning steps.

We present the security evaluation results of RoMa w/o EF, as shown in Fig. 12. Our experiments demonstrate that RoMa w/o EF loses its verifiability after approximately 25 steps and experiences structural collapse of QR positioning squares at around 50 steps. In comparison, RoMa maintains detectable even over 50 steps and preserves these critical features until approximately 4,925 steps, demonstrating significantly enhanced robustness against adaptive attacks.

E More Results about Sensitivity Analysis of the Path-aware Step Size r

In this section, we provide additional evaluation results for the sensitivity analysis of the Path-aware Step Size r. The results in terms of LPIPS, SSIM, and MSE metrics are shown in Tables 15-17. Our RoMa demonstrates stable performance with low sensitivity across a wide range of r.

Table 15: Sensitivity analysis of r in RoMa on MS-COCO-2017 (LPIPS↓).

Method	0k	1k	2k	3k	4k	5k	6k
RoMa(r=0.05)	0.038 ± 0.005	0.061 ± 0.011	0.102 ± 0.066	0.104 ± 0.040	0.192 ± 0.078	0.302 ± 0.127	0.261 ± 0.094
RoMa(r=0.10)	0.037 ± 0.005	0.062 ± 0.011	0.070 ± 0.011	0.151 ± 0.076	0.214 ± 0.073	0.221 ± 0.068	0.267 ± 0.114
RoMa(r=0.30)	0.033 ± 0.005	0.059 ± 0.012	0.070 ± 0.017	0.158 ± 0.085	0.216 ± 0.078	0.219 ± 0.072	0.270 ± 0.113
RoMa(r=0.50)	0.035 ± 0.005	0.062 ± 0.012	0.071 ± 0.012	0.154 ± 0.075	0.216 ± 0.071	0.221 ± 0.066	0.268 ± 0.113
RoMa(r=0.70)	0.034 ± 0.005	0.063 ± 0.013	0.071 ± 0.012	0.156 ± 0.075	0.218 ± 0.071	0.222 ± 0.071	0.266 ± 0.113
RoMa(r=0.90)	0.034 ± 0.004	0.063 ± 0.014	0.075 ± 0.033	0.172 ± 0.089	0.234 ± 0.081	0.237 ± 0.073	0.290 ± 0.114

Table 16: Sensitivity analysis of r in RoMa on MS-COCO-2017 (SSIM↑).

Method	0k	1k	2k	3k	4k	5k	6k
RoMa(r=0.05)	0.886 ± 0.013	0.843 ± 0.041	0.806 ± 0.107	0.785 ± 0.089	0.678 ± 0.139	0.494 ± 0.190	0.590 ± 0.159
RoMa(r=0.10)	0.889 ± 0.013	0.845 ± 0.041	0.857 ± 0.038	0.739 ± 0.129	0.656 ± 0.137	0.631 ± 0.118	0.555 ± 0.167
RoMa(r=0.30)	0.894 ± 0.012	0.857 ± 0.037	0.858 ± 0.046	0.732 ± 0.143	0.659 ± 0.140	0.639 ± 0.125	0.556 ± 0.167
RoMa(r=0.50)	0.892 ± 0.012	0.847 ± 0.040	0.858 ± 0.037	0.737 ± 0.128	0.657 ± 0.132	0.635 ± 0.115	0.557 ± 0.167
RoMa(r=0.70)	0.893 ± 0.012	0.847 ± 0.039	0.856 ± 0.038	0.735 ± 0.127	0.655 ± 0.132	0.632 ± 0.125	0.556 ± 0.166
RoMa(r=0.90)	0.893 ± 0.012	0.851 ± 0.038	0.851 ± 0.057	0.715 ± 0.150	0.635 ± 0.144	0.615 ± 0.128	0.541 ± 0.163

Table 17: Sensitivity analysis of r in RoMa on MS-COCO-2017 (MSE↓).

Method	0k	1k	2k	3k	4k	5k	6k
RoMa(r=0.05)	0.013 ± 0.003	0.020 ± 0.006	0.046 ± 0.047	0.045 ± 0.027	0.106 ± 0.063	0.190 ± 0.103	0.169 ± 0.094
RoMa(r=0.10)	0.012 ± 0.003	0.020 ± 0.007	0.021 ± 0.007	0.077 ± 0.064	0.121 ± 0.070	0.124 ± 0.060	0.173 ± 0.104
RoMa(r=0.30)	0.010 ± 0.002	0.019 ± 0.010	0.021 ± 0.011	0.087 ± 0.079	0.127 ± 0.078	0.127 ± 0.070	0.178 ± 0.108
RoMa(r=0.50)	0.011 ± 0.003	0.020 ± 0.007	0.021 ± 0.007	0.081 ± 0.066	0.124 ± 0.070	0.125 ± 0.058	0.175 ± 0.104
RoMa(r=0.70)	0.011 ± 0.003	0.021 ± 0.008	0.021 ± 0.008	0.082 ± 0.068	0.126 ± 0.071	0.129 ± 0.068	0.174 ± 0.106
RoMa(r=0.90)	0.011 ± 0.002	0.021 ± 0.011	0.024 ± 0.023	0.099 ± 0.086	0.142 ± 0.083	0.143 ± 0.075	0.194 ± 0.108

F Sensitivity Analysis of the Balance Coefficient α

In this section, we provide the sensitivity analysis of α and present the results in terms of LPIPS, SSIM, and MSE metrics, in Tables 18-21. Our experimental results demonstrate that RoMa maintains a relatively stable performance with different α.

Table 18: Sensitivity analysis of α in RoMa on MS-COCO-2017 (LPIPS↓).

Method	0k	1k	2k	3k	4k	5k	6k
SD 1.4	0.858 ± 0.065	0.833 ± 0.058	0.862 ± 0.049	0.838 ± 0.050	0.844 ± 0.066	0.837 ± 0.052	0.839 ± 0.062
WatermarkDM	0.034 ± 0.008	0.153 ± 0.058	0.302 ± 0.108	0.307 ± 0.112	0.342 ± 0.106	0.429 ± 0.128	0.454 ± 0.115
SAM	0.047 ± 0.020	0.161 ± 0.108	0.334 ± 0.142	0.348 ± 0.143	0.419 ± 0.144	0.452 ± 0.137	0.431 ± 0.129
RoMa w/o PS	0.031 ± 0.005	0.093 ± 0.039	0.239 ± 0.113	0.275 ± 0.115	0.330 ± 0.108	0.392 ± 0.107	0.407 ± 0.120
RoMa w/o EF	0.046 ± 0.014	0.184 ± 0.111	0.339 ± 0.133	0.325 ± 0.147	0.457 ± 0.127	0.454 ± 0.132	0.448 ± 0.136
RoMa(α=0.36)	0.038 ± 0.005	0.076 ± 0.013	0.128 ± 0.087	0.140 ± 0.055	0.198 ± 0.073	0.296 ± 0.113	0.302 ± 0.113
RoMa(α=0.38)	0.031 ± 0.004	0.062 ± 0.011	0.125 ± 0.091	0.143 ± 0.068	0.191 ± 0.090	0.291 ± 0.114	0.299 ± 0.113
RoMa(α=0.40)	0.038 ± 0.005	0.061 ± 0.011	0.102 ± 0.066	0.104 ± 0.040	0.192 ± 0.078	0.302 ± 0.127	0.261 ± 0.094
RoMa(α=0.42)	0.033 ± 0.005	0.055 ± 0.010	0.082 ± 0.056	0.099 ± 0.032	0.152 ± 0.064	0.256 ± 0.117	0.249 ± 0.105
RoMa(α=0.44)	0.030 ± 0.004	0.057 ± 0.010	0.109 ± 0.074	0.115 ± 0.050	0.165 ± 0.078	0.270 ± 0.118	0.259 ± 0.104

Table 19: Sensitivity analysis of α in RoMa on MS-COCO-2017 (SSIM↑).

Method	0k	1k	2k	3k	4k	5k	6k
SD 1.4	0.098 ± 0.047	0.095 ± 0.049	0.106 ± 0.057	0.102 ± 0.051	0.098 ± 0.056	0.090 ± 0.051	0.100 ± 0.055
WatermarkDM	0.904 ± 0.014	0.772 ± 0.094	0.545 ± 0.176	0.524 ± 0.177	0.458 ± 0.169	0.343 ± 0.173	0.343 ± 0.153
SAM	0.868 ± 0.030	0.694 ± 0.180	0.451 ± 0.224	0.428 ± 0.212	0.333 ± 0.197	0.280 ± 0.186	0.322 ± 0.182
RoMa w/o PS	0.901 ± 0.013	0.825 ± 0.063	0.643 ± 0.172	0.574 ± 0.184	0.499 ± 0.174	0.397 ± 0.171	0.421 ± 0.166
RoMa w/o EF	0.867 ± 0.029	0.682 ± 0.173	0.456 ± 0.201	0.453 ± 0.217	0.288 ± 0.162	0.274 ± 0.174	0.313 ± 0.173
RoMa(α=0.36)	0.885 ± 0.012	0.840 ± 0.031	0.783 ± 0.132	0.759 ± 0.103	0.686 ± 0.132	0.518 ± 0.185	0.534 ± 0.184
RoMa(α=0.38)	0.899 ± 0.010	0.861 ± 0.031	0.782 ± 0.143	0.752 ± 0.126	0.693 ± 0.159	0.523 ± 0.189	0.549 ± 0.180
RoMa(α=0.40)	0.886 ± 0.013	0.843 ± 0.041	0.806 ± 0.107	0.785 ± 0.089	0.678 ± 0.139	0.494 ± 0.190	0.590 ± 0.159
RoMa(α=0.42)	0.895 ± 0.011	0.860 ± 0.034	0.834 ± 0.091	0.806 ± 0.079	0.739 ± 0.122	0.559 ± 0.187	0.605 ± 0.178
RoMa(α=0.44)	0.902 ± 0.011	0.869 ± 0.028	0.804 ± 0.121	0.790 ± 0.100	0.723 ± 0.143	0.539 ± 0.195	0.606 ± 0.173

Table 20: Sensitivity analysis of α in RoMa on MS-COCO-2017 (MSE↓).

Method	0k	1k	2k	3k	4k	5k	6k
SD 1.4	0.304 ± 0.036	0.310 ± 0.036	0.298 ± 0.031	0.306 ± 0.034	0.309 ± 0.037	0.311 ± 0.036	0.308 ± 0.036
WatermarkDM	0.009 ± 0.004	0.083 ± 0.061	0.211 ± 0.105	0.205 ± 0.092	0.242 ± 0.089	0.299 ± 0.097	0.329 ± 0.087
SAM	0.019 ± 0.017	0.101 ± 0.102	0.249 ± 0.131	0.241 ± 0.121	0.291 ± 0.109	0.321 ± 0.110	0.321 ± 0.115
RoMa w/o PS	0.009 ± 0.002	0.036 ± 0.029	0.163 ± 0.113	0.182 ± 0.109	0.241 ± 0.113	0.293 ± 0.113	0.301 ± 0.106
RoMa w/o EF	0.017 ± 0.012	0.118 ± 0.111	0.259 ± 0.126	0.223 ± 0.127	0.324 ± 0.097	0.323 ± 0.105	0.318 ± 0.105
RoMa(α=0.36)	0.012 ± 0.002	0.027 ± 0.008	0.065 ± 0.069	0.066 ± 0.044	0.107 ± 0.061	0.195 ± 0.110	0.211 ± 0.116
RoMa(α=0.38)	0.009 ± 0.002	0.018 ± 0.007	0.070 ± 0.082	0.073 ± 0.059	0.111 ± 0.082	0.206 ± 0.122	0.215 ± 0.120
RoMa(α=0.40)	0.013 ± 0.003	0.020 ± 0.006	0.046 ± 0.047	0.045 ± 0.027	0.106 ± 0.063	0.190 ± 0.103	0.169 ± 0.094
RoMa(α=0.42)	0.010 ± 0.002	0.016 ± 0.005	0.035 ± 0.042	0.041 ± 0.022	0.075 ± 0.049	0.161 ± 0.106	0.162 ± 0.106
RoMa(α=0.44)	0.009 ± 0.002	0.015 ± 0.007	0.054 ± 0.062	0.053 ± 0.040	0.091 ± 0.070	0.183 ± 0.117	0.178 ± 0.112

Table 21: Sensitivity analysis of α in RoMa on MS-COCO-2017 (SCORE↑).

Method	0k	1k	2k	3k	4k	5k	6k
SD 1.4	0.239 ± 0.032	0.250 ± 0.031	0.242 ± 0.029	0.250 ± 0.027	0.246 ± 0.034	0.246 ± 0.029	0.249 ± 0.034
WatermarkDM	0.952 ± 0.008	0.838 ± 0.068	0.670 ± 0.126	0.663 ± 0.125	0.618 ± 0.118	0.529 ± 0.130	0.510 ± 0.115
SAM	0.933 ± 0.022	0.808 ± 0.127	0.618 ± 0.162	0.606 ± 0.156	0.532 ± 0.149	0.494 ± 0.140	0.517 ± 0.137
RoMa w/o PS	0.953 ± 0.006	0.894 ± 0.041	0.741 ± 0.130	0.698 ± 0.133	0.636 ± 0.127	0.565 ± 0.124	0.563 ± 0.127
RoMa w/o EF	0.934 ± 0.017	0.789 ± 0.128	0.616 ± 0.149	0.629 ± 0.160	0.493 ± 0.127	0.491 ± 0.132	0.507 ± 0.134
RoMa(α=0.36)	0.944 ± 0.006	0.909 ± 0.014	0.858 ± 0.096	0.844 ± 0.065	0.785 ± 0.087	0.668 ± 0.132	0.667 ± 0.133
RoMa(α=0.38)	0.952 ± 0.006	0.924 ± 0.013	0.858 ± 0.104	0.839 ± 0.081	0.790 ± 0.108	0.670 ± 0.136	0.672 ± 0.132
RoMa(α=0.40)	0.944 ± 0.007	0.919 ± 0.015	0.882 ± 0.074	0.875 ± 0.049	0.786 ± 0.092	0.659 ± 0.139	0.713 ± 0.112
RoMa(α=0.42)	0.950 ± 0.006	0.928 ± 0.012	0.902 ± 0.062	0.884 ± 0.041	0.831 ± 0.077	0.708 ± 0.134	0.724 ± 0.125
RoMa(α=0.44)	0.954 ± 0.006	0.929 ± 0.012	0.876 ± 0.085	0.869 ± 0.061	0.816 ± 0.095	0.690 ± 0.139	0.717 ± 0.125

G Sensitivity Analysis of SAM's Perturbation Scale ϵ

In our primary experiments, we set the perturbation scale ϵ of SAM to 0.01. To investigate the impact of ϵ on watermark robustness, we conduct ablation experiments on the MS-COCO-2017 dataset with varying ϵ values of 0.02 and 0.05, following prior research [16]. Our experimental results (presented in Tables 22-25) indicate that despite increasing ϵ, we do not observe a significant enhancement in watermark robustness against fine-tuning. Furthermore, as ϵ reaches 0.05, the watermark SCORE notably decreases, averaging only 0.688 even without further fine-tuning (column "0k"). This is likely attributed to the larger ϵ compromising the original watermark embedding functionality. In sum, these analyses further support our conclusion in Section 6.1: path-specific smoothness proves more effective than SAM for enhancing watermark robustness against fine-tuning.

Table 22: Sensitivity analysis of ϵ in SAM on MS-COCO-2017 (LPIPS↓ metric).

Method	0k	1k	2k	3k	4k	5k	6k
SAM(ϵ=0.01)	0.047 ± 0.020	0.161 ± 0.108	0.334 ± 0.142	0.348 ± 0.143	0.419 ± 0.144	0.452 ± 0.137	0.431 ± 0.129
SAM(ϵ=0.02)	0.057 ± 0.022	0.193 ± 0.100	0.355 ± 0.116	0.362 ± 0.124	0.439 ± 0.117	0.492 ± 0.131	0.406 ± 0.095
SAM(ϵ=0.05)	0.277 ± 0.046	0.349 ± 0.053	0.400 ± 0.064	0.398 ± 0.059	0.399 ± 0.057	0.425 ± 0.069	0.416 ± 0.057
RoMa	0.038 ± 0.005	0.061 ± 0.011	0.102 ± 0.066	0.104 ± 0.040	0.192 ± 0.078	0.302 ± 0.127	0.261 ± 0.094

Table 23: Sensitivity analysis of ϵ in SAM on MS-COCO-2017 (SSIM↑).

Method	0k	1k	2k	3k	4k	5k	6k
SAM(ϵ=0.01)	0.868 ± 0.030	0.694 ± 0.180	0.451 ± 0.224	0.428 ± 0.212	0.333 ± 0.197	0.280 ± 0.186	0.322 ± 0.182
SAM(ϵ=0.02)	0.853 ± 0.042	0.641 ± 0.171	0.423 ± 0.184	0.390 ± 0.190	0.292 ± 0.169	0.224 ± 0.151	0.346 ± 0.156
SAM(ϵ=0.05)	0.559 ± 0.079	0.418 ± 0.102	0.321 ± 0.098	0.318 ± 0.105	0.318 ± 0.105	0.273 ± 0.099	0.306 ± 0.093
RoMa	0.886 ± 0.013	0.843 ± 0.041	0.806 ± 0.107	0.785 ± 0.089	0.678 ± 0.139	0.494 ± 0.190	0.590 ± 0.159

Table 24: Sensitivity analysis of ϵ in SAM on MS-COCO-2017 (MSE↓).

Method	0k	1k	2k	3k	4k	5k	6k
SAM(ϵ=0.01)	0.019 ± 0.017	0.101 ± 0.102	0.249 ± 0.131	0.241 ± 0.121	0.291 ± 0.109	0.321 ± 0.110	0.321 ± 0.115
SAM(ϵ=0.02)	0.025 ± 0.018	0.134 ± 0.102	0.278 ± 0.113	0.268 ± 0.116	0.330 ± 0.098	0.334 ± 0.086	0.330 ± 0.104
SAM(ϵ=0.05)	0.208 ± 0.052	0.303 ± 0.078	0.352 ± 0.072	0.344 ± 0.076	0.352 ± 0.079	0.363 ± 0.073	0.372 ± 0.070
RoMa	0.013 ± 0.003	0.020 ± 0.006	0.046 ± 0.047	0.045 ± 0.027	0.106 ± 0.063	0.190 ± 0.103	0.169 ± 0.094

Table 25: Sensitivity analysis of ϵ in SAM on MS-COCO-2017 (SCORE↑).

Method	0k	1k	2k	3k	4k	5k	6k
SAM(ϵ=0.01)	0.933 ± 0.022	0.808 ± 0.127	0.618 ± 0.162	0.606 ± 0.156	0.532 ± 0.149	0.494 ± 0.140	0.517 ± 0.137
SAM(ϵ=0.02)	0.922 ± 0.026	0.769 ± 0.120	0.594 ± 0.133	0.583 ± 0.138	0.502 ± 0.124	0.454 ± 0.120	0.535 ± 0.110
SAM(ϵ=0.05)	0.688 ± 0.056	0.591 ± 0.071	0.526 ± 0.071	0.528 ± 0.071	0.526 ± 0.072	0.497 ± 0.071	0.509 ± 0.065
RoMa	0.944 ± 0.007	0.919 ± 0.015	0.882 ± 0.074	0.875 ± 0.049	0.786 ± 0.092	0.659 ± 0.139	0.713 ± 0.112

H Implementation Details of Watermark Detection

Stable Signature [13] and AquaLora [12] embed a k-bit binary signature $m \in \{0,1\}^k$ into generated images. For watermark detection, they first utilize the watermark extractor to decode a message m' from a candidate image x and compare it with the predefined signature m. The detection mechanism relies on testing the statistical hypothesis H_1: x was generated by the watermarked model against the null hypothesis H_0: x was not generated by the watermarked model. Specifically, they set a bit threshold τ and reject the null hypothesis H_0 when the number of matched bits $M(m, m')$ between the extracted message m' and the signature m satisfies:

$$M(m, m') \geq \tau \text{ where } \tau \in \{0, \ldots, k\}. \tag{3}$$

To obtain the False Positive Rate (FPR) associated with each bit threshold τ, they assume the extracted bits follow an i.i.d. Bernoulli distribution with parameter 0.5 under H_0 (i.e., random guess between bit 0 and 1). This yields a binomial distribution for $M(m, m')$, with parameters $(k, 0.5)$. The FPR can then be formulated as:

$$\text{FPR}(\tau) = \mathbb{P}(M > \tau | H_0) = \sum_{i=\tau+1}^{k} \binom{k}{i} \frac{1}{2^k}. \tag{4}$$

I Experimental Setup for Stable Signature

Stable Signature [13] embeds watermarks into the Variational Autoencoder (VAE) decoder, so that all generated images carry binary messages. We follow the experimental settings of prior

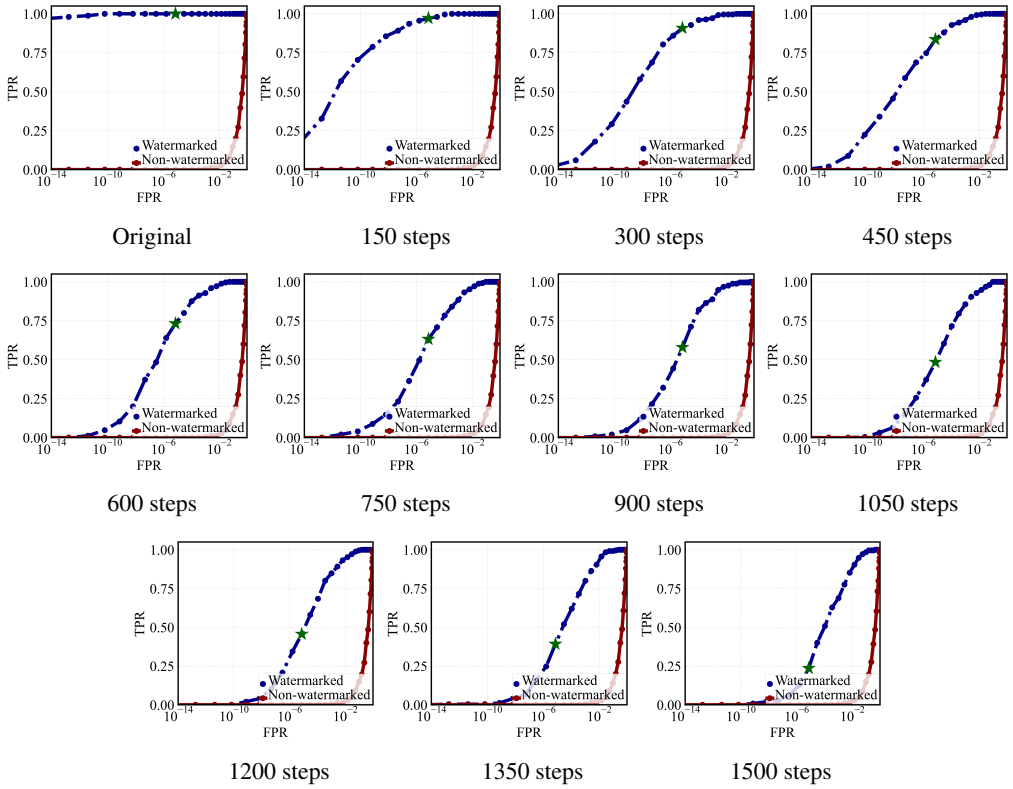

Figure 13: ROC curves of Stable Signature at various fine-tuning steps. The star with green color ($\star$) is highlighted (FPR $= 10^{-6}$) where its associated TPR reflects the detection accuracy with $\tau = 38$.

studies [13, 23, 58], and fine-tune the latent decoder to evaluate its robustness. Specifically, we use the MS-COCO-2017 validation set, randomly selecting 4,000 images for fine-tuning and reserving the remaining 1,000 images for evaluation. The fine-tuning process only minimizes the LPIPS loss between the original image and the image reconstructed by the latent decoder (as this maintains higher generation quality, following [58]), with a learning rate of 1×10^{-4}. For the watermarked model, we use the official checkpoint[8], which embeds a 48-bit binary message into the generated images. We set the bit threshold to $\tau = 38$ (FPR $= 10^{-6}$) for watermark detection.

J Experimental Setup for AquaLora

AquaLora [12] also embeds binary messages into all generated images. However, it differs in that it merges watermark information into the U-Net [46, 20, 45] using Low Rank Adaptation (LoRA) [51] through a scaling matrix strategy, thereby enabling watermark embedding during the denoising process. We evaluate the robustness of AquaLora against fine-tuning on the MS-COCO-2017 and CUB-200-2011 datasets, respectively, adopting the same fine-tuning protocol as described in the *Robustness Evaluation* section (Section 5.3). For the watermarked model, we first obtain the official prior-preserving fine-tuned checkpoints[9], and then embed the same 48-bit message as in Stable Signature into Stable Diffusion v1.5[10] with LoRA rank $= 320$. Here, we still set the bit threshold to $\tau = 38$ (FPR $= 10^{-6}$) for watermark detection [13, 58]. We use the prompt templates provided by AquaLora[11] for image generation, with the original Stable Diffusion v1.5 serving as the non-watermarked reference.

[8] https://github.com/facebookresearch/stable_signature
[9] https://huggingface.co/georgefen/AquaLoRA-Models/tree/main/ppft_trained
[10] https://huggingface.co/stable-diffusion-v1-5/stable-diffusion-v1-5/tree/main
[11] https://github.com/Georgefwt/AquaLoRA/tree/master/evaluation

Figure 14: Visual comparison between original images (top) and their reconstructions by Stable Signature's watermarked decoder (bottom).

Figure 15: Visual comparison between original images (top) and reconstructions by Stable Signature's watermarked decoder after 1500 fine-tuning steps (bottom).

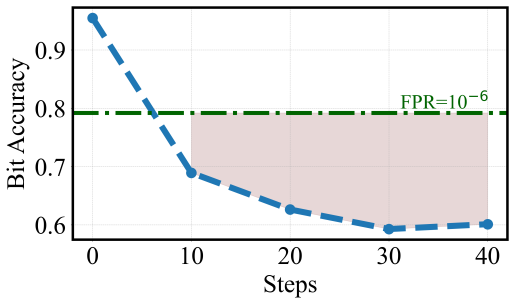

Figure 16: Bit accuracy results of AquaLora against the fine-tuning process on CUB-200-2011 dataset.

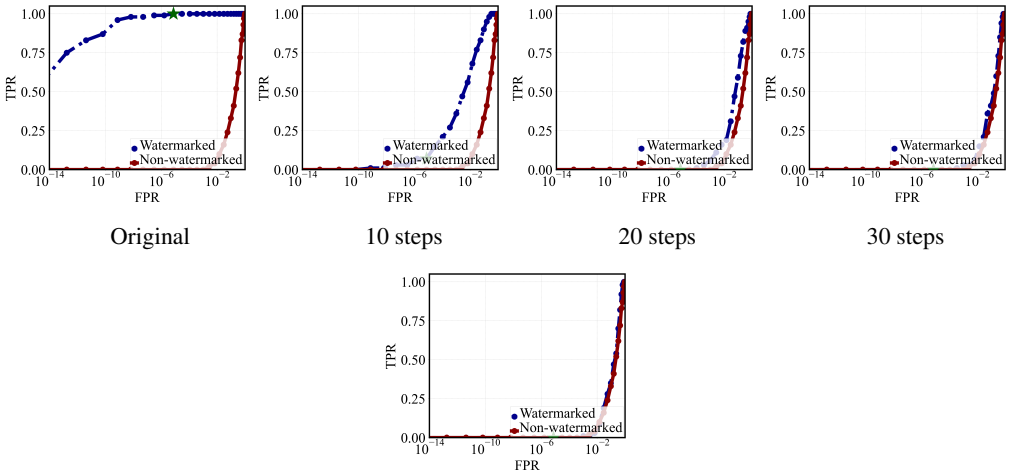

Original 10 steps 20 steps 30 steps

40 steps

Figure 17: ROC curves of AquaLora at various fine-tuning steps on MS-COCO-2017 dataset. The star with green color ($\star$) is highlighted (FPR $= 10^{-6}$) where its associated TPR reflects the detection accuracy with $\tau = 38$.

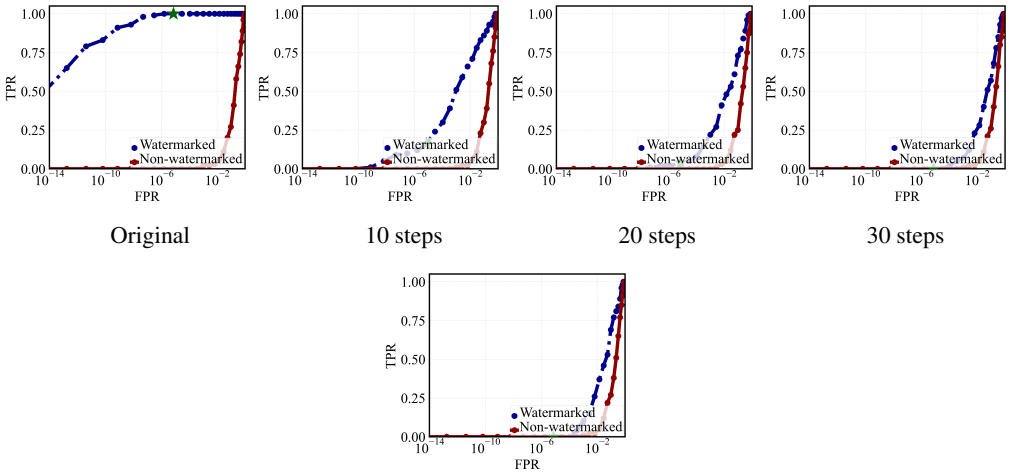

Original 10 steps 20 steps 30 steps

40 steps

Figure 18: ROC curves of AquaLora at various fine-tuning steps on CUB-200-2011 dataset. The star with green color ($\star$) is highlighted (FPR $= 10^{-6}$) where its associated TPR reflects the detection accuracy with $\tau = 38$.

K Additional Discussions of Diffusion Models

Diffusion models [20, 39, 19, 45, 41, 52, 64] have emerged as powerful generative paradigms, demonstrating remarkable success across various domains, including high-quality image synthesis [9, 47, 67], video generation [21, 60, 62], and natural language generation [31]. While our work focuses on protecting the watermarking robustness on Text-to-Image (T2I) diffusion models, our proposed RoMa is general and can be potentially adapted to watermarking diffusion models with different generative tasks [34, 25], and architectures [40].

L Discussion on Robustness Against Various Watermark Removal Attacks

In this section, we provide a comprehensive discussion on RoMa's robustness against various types of watermark removal attacks, addressing concerns raised about the scope of our evaluation.

L.1 Image-Level Attacks

Unlike embedding watermarks into the generated images, RoMa is a trigger-based watermark that operates by rooting watermark information within the parameter space. As such, RoMa can defend against image-level watermark attacks such as compression, rotation, cropping, denoising reconstruction, etc. [13, 69, 12, 29].

L.2 Model-Level Removal Attacks

For model-level removal attacks, we have extensively evaluated RoMa's robustness in our main experiments. As demonstrated in Section 6.1, RoMa maintains strong watermark preservation under standard fine-tuning scenarios (our primary threat model) across different datasets, i.e., MS-COCO-2017 and CUB-200-2011, for up to 6,000 fine-tuning steps, significantly outperforming existing baselines. Furthermore, in Section 6.3, we evaluate RoMa against adaptive fine-tuning attacks, a strong removal attack where we assume attackers possess watermark knowledge and deliberately attempt to unlearn the watermark using synthetically generated unlearning data. Our experimental results show that even under such rigorous conditions, RoMa maintains strong defense capabilities, demonstrating excellent robustness against both vanilla and adaptive fine-tuning paradigms.

L.3 Model Distillation Attacks

Beyond fine-tuning attacks, an attacker could theoretically attempt to distill a new model from our watermarked model to bypass watermark detection. In such a distillation attack scenario, the attacker would train a student model using synthetic data generated from our watermarked model, aiming to replicate the generation capability while excluding the watermark trigger from the training data. However, there still exist fundamental limitations that restrict the practicality of such distillation attacks in real-world scenarios. In practice, most distillation processes begin from an existing base model rather than training entirely from scratch. This is because training a large-scale generative model such as Stable Diffusion from scratch is prohibitively expensive, making it impractical for most users. Additionally, training from scratch using only synthetic data from our target model is often highly unstable due to the biased synthetic dataset [2], leading to degraded image quality [48, 53, 49]. Indeed, the emphasized distillation scenario exactly highlights the practical significance of our model watermarking. Our primary threat model focuses on protecting the intellectual property of our released base models. That is to say, if an attacker fine-tunes or distills a new model from our base model, our backdoor-based watermark remains embedded in the model's parameters. This allows us to reliably detect unauthorized use of our model.

M Limitations

While extensive fine-tuning (e.g., over 6,000 steps) may eventually impact watermark detection, our approach significantly extends the robustness boundary compared to existing methods that are vulnerable even after just 1,000 fine-tuning steps. Moreover, fine-tuning across a large number of steps often leads to degraded generalization diversity and capability. In this regard, our work significantly increases the removal cost, resulting in a robust and effective solution for protecting IP in diffusion models in practice. Furthermore, we believe that this work will spark fruitful discussions and pave the way for future work on developing robust watermarking schemes in generative models.

NeurIPS Paper Checklist

The checklist is designed to encourage best practices for responsible machine learning research, addressing issues of reproducibility, transparency, research ethics, and societal impact. Do not remove the checklist: **The papers not including the checklist will be desk rejected.** The checklist should follow the references and follow the (optional) supplemental material. The checklist does NOT count towards the page limit.

Please read the checklist guidelines carefully for information on how to answer these questions. For each question in the checklist:

- You should answer [Yes] , [No] , or [NA] .
- [NA] means either that the question is Not Applicable for that particular paper or the relevant information is Not Available.
- Please provide a short (1–2 sentence) justification right after your answer (even for NA).

The checklist answers are an integral part of your paper submission. They are visible to the reviewers, area chairs, senior area chairs, and ethics reviewers. You will be asked to also include it (after eventual revisions) with the final version of your paper, and its final version will be published with the paper.

The reviewers of your paper will be asked to use the checklist as one of the factors in their evaluation. While "[Yes] " is generally preferable to "[No] ", it is perfectly acceptable to answer "[No] " provided a proper justification is given (e.g., "error bars are not reported because it would be too computationally expensive" or "we were unable to find the license for the dataset we used"). In general, answering "[No] " or "[NA] " is not grounds for rejection. While the questions are phrased in a binary way, we acknowledge that the true answer is often more nuanced, so please just use your best judgment and write a justification to elaborate. All supporting evidence can appear either in the main paper or the supplemental material, provided in appendix. If you answer [Yes] to a question, in the justification please point to the section(s) where related material for the question can be found.

IMPORTANT, please:

- **Delete this instruction block, but keep the section heading "NeurIPS Paper Checklist"**,
- **Keep the checklist subsection headings, questions/answers and guidelines below.**
- **Do not modify the questions and only use the provided macros for your answers**.

1. **Claims**

   Question: Do the main claims made in the abstract and introduction accurately reflect the paper's contributions and scope?

   Answer: [Yes]

   Justification: Please see our description in the abstract and introduction.

   Guidelines:

   - The answer NA means that the abstract and introduction do not include the claims made in the paper.
   - The abstract and/or introduction should clearly state the claims made, including the contributions made in the paper and important assumptions and limitations. A No or NA answer to this question will not be perceived well by the reviewers.
   - The claims made should match theoretical and experimental results, and reflect how much the results can be expected to generalize to other settings.
   - It is fine to include aspirational goals as motivation as long as it is clear that these goals are not attained by the paper.

2. **Limitations**

   Question: Does the paper discuss the limitations of the work performed by the authors?

   Answer: [Yes]

   Justification: We discuss limitations in the conclusion.

Guidelines:

- The answer NA means that the paper has no limitation while the answer No means that the paper has limitations, but those are not discussed in the paper.
- The authors are encouraged to create a separate "Limitations" section in their paper.
- The paper should point out any strong assumptions and how robust the results are to violations of these assumptions (e.g., independence assumptions, noiseless settings, model well-specification, asymptotic approximations only holding locally). The authors should reflect on how these assumptions might be violated in practice and what the implications would be.
- The authors should reflect on the scope of the claims made, e.g., if the approach was only tested on a few datasets or with a few runs. In general, empirical results often depend on implicit assumptions, which should be articulated.
- The authors should reflect on the factors that influence the performance of the approach. For example, a facial recognition algorithm may perform poorly when image resolution is low or images are taken in low lighting. Or a speech-to-text system might not be used reliably to provide closed captions for online lectures because it fails to handle technical jargon.
- The authors should discuss the computational efficiency of the proposed algorithms and how they scale with dataset size.
- If applicable, the authors should discuss possible limitations of their approach to address problems of privacy and fairness.
- While the authors might fear that complete honesty about limitations might be used by reviewers as grounds for rejection, a worse outcome might be that reviewers discover limitations that aren't acknowledged in the paper. The authors should use their best judgment and recognize that individual actions in favor of transparency play an important role in developing norms that preserve the integrity of the community. Reviewers will be specifically instructed to not penalize honesty concerning limitations.

3. **Theory assumptions and proofs**

   Question: For each theoretical result, does the paper provide the full set of assumptions and a complete (and correct) proof?

   Answer: [Yes]

   Justification: NA

   Guidelines:

   - The answer NA means that the paper does not include theoretical results.
   - All the theorems, formulas, and proofs in the paper should be numbered and cross-referenced.
   - All assumptions should be clearly stated or referenced in the statement of any theorems.
   - The proofs can either appear in the main paper or the supplemental material, but if they appear in the supplemental material, the authors are encouraged to provide a short proof sketch to provide intuition.
   - Inversely, any informal proof provided in the core of the paper should be complemented by formal proofs provided in appendix or supplemental material.
   - Theorems and Lemmas that the proof relies upon should be properly referenced.

4. **Experimental result reproducibility**

   Question: Does the paper fully disclose all the information needed to reproduce the main experimental results of the paper to the extent that it affects the main claims and/or conclusions of the paper (regardless of whether the code and data are provided or not)?

   Answer: [Yes]

   Justification: Please refer to our experimental setting.

   Guidelines:

   - The answer NA means that the paper does not include experiments.

- If the paper includes experiments, a No answer to this question will not be perceived well by the reviewers: Making the paper reproducible is important, regardless of whether the code and data are provided or not.
- If the contribution is a dataset and/or model, the authors should describe the steps taken to make their results reproducible or verifiable.
- Depending on the contribution, reproducibility can be accomplished in various ways. For example, if the contribution is a novel architecture, describing the architecture fully might suffice, or if the contribution is a specific model and empirical evaluation, it may be necessary to either make it possible for others to replicate the model with the same dataset, or provide access to the model. In general. releasing code and data is often one good way to accomplish this, but reproducibility can also be provided via detailed instructions for how to replicate the results, access to a hosted model (e.g., in the case of a large language model), releasing of a model checkpoint, or other means that are appropriate to the research performed.
- While NeurIPS does not require releasing code, the conference does require all submissions to provide some reasonable avenue for reproducibility, which may depend on the nature of the contribution. For example
  (a) If the contribution is primarily a new algorithm, the paper should make it clear how to reproduce that algorithm.
  (b) If the contribution is primarily a new model architecture, the paper should describe the architecture clearly and fully.
  (c) If the contribution is a new model (e.g., a large language model), then there should either be a way to access this model for reproducing the results or a way to reproduce the model (e.g., with an open-source dataset or instructions for how to construct the dataset).
  (d) We recognize that reproducibility may be tricky in some cases, in which case authors are welcome to describe the particular way they provide for reproducibility. In the case of closed-source models, it may be that access to the model is limited in some way (e.g., to registered users), but it should be possible for other researchers to have some path to reproducing or verifying the results.

5. **Open access to data and code**

   Question: Does the paper provide open access to the data and code, with sufficient instructions to faithfully reproduce the main experimental results, as described in supplemental material?

   Answer: [Yes]

   Justification:

   Guidelines:

   - The answer NA means that paper does not include experiments requiring code.
   - Please see the NeurIPS code and data submission guidelines (https://nips.cc/public/guides/CodeSubmissionPolicy) for more details.
   - While we encourage the release of code and data, we understand that this might not be possible, so "No" is an acceptable answer. Papers cannot be rejected simply for not including code, unless this is central to the contribution (e.g., for a new open-source benchmark).
   - The instructions should contain the exact command and environment needed to run to reproduce the results. See the NeurIPS code and data submission guidelines (https://nips.cc/public/guides/CodeSubmissionPolicy) for more details.
   - The authors should provide instructions on data access and preparation, including how to access the raw data, preprocessed data, intermediate data, and generated data, etc.
   - The authors should provide scripts to reproduce all experimental results for the new proposed method and baselines. If only a subset of experiments are reproducible, they should state which ones are omitted from the script and why.
   - At submission time, to preserve anonymity, the authors should release anonymized versions (if applicable).

- Providing as much information as possible in supplemental material (appended to the paper) is recommended, but including URLs to data and code is permitted.

6. **Experimental setting/details**

   Question: Does the paper specify all the training and test details (e.g., data splits, hyperparameters, how they were chosen, type of optimizer, etc.) necessary to understand the results?

   Answer: [Yes]

   Justification: Please refer to our experimental setting.

   Guidelines:

   - The answer NA means that the paper does not include experiments.
   - The experimental setting should be presented in the core of the paper to a level of detail that is necessary to appreciate the results and make sense of them.
   - The full details can be provided either with the code, in appendix, or as supplemental material.

7. **Experiment statistical significance**

   Question: Does the paper report error bars suitably and correctly defined or other appropriate information about the statistical significance of the experiments?

   Answer: [Yes]

   Justification: Section 6.

   Guidelines:

   - The answer NA means that the paper does not include experiments.
   - The authors should answer "Yes" if the results are accompanied by error bars, confidence intervals, or statistical significance tests, at least for the experiments that support the main claims of the paper.
   - The factors of variability that the error bars are capturing should be clearly stated (for example, train/test split, initialization, random drawing of some parameter, or overall run with given experimental conditions).
   - The method for calculating the error bars should be explained (closed form formula, call to a library function, bootstrap, etc.)
   - The assumptions made should be given (e.g., Normally distributed errors).
   - It should be clear whether the error bar is the standard deviation or the standard error of the mean.
   - It is OK to report 1-sigma error bars, but one should state it. The authors should preferably report a 2-sigma error bar than state that they have a 96% CI, if the hypothesis of Normality of errors is not verified.
   - For asymmetric distributions, the authors should be careful not to show in tables or figures symmetric error bars that would yield results that are out of range (e.g. negative error rates).
   - If error bars are reported in tables or plots, The authors should explain in the text how they were calculated and reference the corresponding figures or tables in the text.

8. **Experiments compute resources**

   Question: For each experiment, does the paper provide sufficient information on the computer resources (type of compute workers, memory, time of execution) needed to reproduce the experiments?

   Answer: [Yes]

   Justification: Section 5.3.

   Guidelines:

   - The answer NA means that the paper does not include experiments.
   - The paper should indicate the type of compute workers CPU or GPU, internal cluster, or cloud provider, including relevant memory and storage.

- The paper should provide the amount of compute required for each of the individual experimental runs as well as estimate the total compute.
- The paper should disclose whether the full research project required more compute than the experiments reported in the paper (e.g., preliminary or failed experiments that didn't make it into the paper).

9. **Code of ethics**

   Question: Does the research conducted in the paper conform, in every respect, with the NeurIPS Code of Ethics https://neurips.cc/public/EthicsGuidelines?

   Answer: [Yes]

   Justification: We thoroughly read the NeurIPS Code of Ethics.

   Guidelines:

   - The answer NA means that the authors have not reviewed the NeurIPS Code of Ethics.
   - If the authors answer No, they should explain the special circumstances that require a deviation from the Code of Ethics.
   - The authors should make sure to preserve anonymity (e.g., if there is a special consideration due to laws or regulations in their jurisdiction).

10. **Broader impacts**

    Question: Does the paper discuss both potential positive societal impacts and negative societal impacts of the work performed?

    Answer: [Yes]

    Justification: We protect the intellectual property of diffusion models, which helps safeguard the usage of diffusion models.

    Guidelines:

    - The answer NA means that there is no societal impact of the work performed.
    - If the authors answer NA or No, they should explain why their work has no societal impact or why the paper does not address societal impact.
    - Examples of negative societal impacts include potential malicious or unintended uses (e.g., disinformation, generating fake profiles, surveillance), fairness considerations (e.g., deployment of technologies that could make decisions that unfairly impact specific groups), privacy considerations, and security considerations.
    - The conference expects that many papers will be foundational research and not tied to particular applications, let alone deployments. However, if there is a direct path to any negative applications, the authors should point it out. For example, it is legitimate to point out that an improvement in the quality of generative models could be used to generate deepfakes for disinformation. On the other hand, it is not needed to point out that a generic algorithm for optimizing neural networks could enable people to train models that generate Deepfakes faster.
    - The authors should consider possible harms that could arise when the technology is being used as intended and functioning correctly, harms that could arise when the technology is being used as intended but gives incorrect results, and harms following from (intentional or unintentional) misuse of the technology.
    - If there are negative societal impacts, the authors could also discuss possible mitigation strategies (e.g., gated release of models, providing defenses in addition to attacks, mechanisms for monitoring misuse, mechanisms to monitor how a system learns from feedback over time, improving the efficiency and accessibility of ML).

11. **Safeguards**

    Question: Does the paper describe safeguards that have been put in place for responsible release of data or models that have a high risk for misuse (e.g., pretrained language models, image generators, or scraped datasets)?

    Answer: [NA]

    Justification:

    Guidelines:

- The answer NA means that the paper poses no such risks.
- Released models that have a high risk for misuse or dual-use should be released with necessary safeguards to allow for controlled use of the model, for example by requiring that users adhere to usage guidelines or restrictions to access the model or implementing safety filters.
- Datasets that have been scraped from the Internet could pose safety risks. The authors should describe how they avoided releasing unsafe images.
- We recognize that providing effective safeguards is challenging, and many papers do not require this, but we encourage authors to take this into account and make a best faith effort.

12. **Licenses for existing assets**

    Question: Are the creators or original owners of assets (e.g., code, data, models), used in the paper, properly credited and are the license and terms of use explicitly mentioned and properly respected?

    Answer: [Yes]

    Justification: Section 1.

    Guidelines:

    - The answer NA means that the paper does not use existing assets.
    - The authors should cite the original paper that produced the code package or dataset.
    - The authors should state which version of the asset is used and, if possible, include a URL.
    - The name of the license (e.g., CC-BY 4.0) should be included for each asset.
    - For scraped data from a particular source (e.g., website), the copyright and terms of service of that source should be provided.
    - If assets are released, the license, copyright information, and terms of use in the package should be provided. For popular datasets, `paperswithcode.com/datasets` has curated licenses for some datasets. Their licensing guide can help determine the license of a dataset.
    - For existing datasets that are re-packaged, both the original license and the license of the derived asset (if it has changed) should be provided.
    - If this information is not available online, the authors are encouraged to reach out to the asset's creators.

13. **New assets**

    Question: Are new assets introduced in the paper well documented and is the documentation provided alongside the assets?

    Answer: [NA]

    Justification:

    Guidelines:

    - The answer NA means that the paper does not release new assets.
    - Researchers should communicate the details of the dataset/code/model as part of their submissions via structured templates. This includes details about training, license, limitations, etc.
    - The paper should discuss whether and how consent was obtained from people whose asset is used.
    - At submission time, remember to anonymize your assets (if applicable). You can either create an anonymized URL or include an anonymized zip file.

14. **Crowdsourcing and research with human subjects**

    Question: For crowdsourcing experiments and research with human subjects, does the paper include the full text of instructions given to participants and screenshots, if applicable, as well as details about compensation (if any)?

    Answer: [NA]

Justification:

Guidelines:

- The answer NA means that the paper does not involve crowdsourcing nor research with human subjects.
- Including this information in the supplemental material is fine, but if the main contribution of the paper involves human subjects, then as much detail as possible should be included in the main paper.
- According to the NeurIPS Code of Ethics, workers involved in data collection, curation, or other labor should be paid at least the minima wage in the country of the data collector.

15. **Institutional review board (IRB) approvals or equivalent for research with human subjects**

    Question: Does the paper describe potential risks incurred by study participants, whether such risks were disclosed to the subjects, and whether Institutional Review Board (IRB) approvals (or an equivalent approval/review based on the requirements of your country or institution) were obtained?

    Answer: [NA]

    Justification:

    Guidelines:

    - The answer NA means that the paper does not involve crowdsourcing nor research with human subjects.
    - Depending on the country in which research is conducted, IRB approval (or equivalent) may be required for any human subjects research. If you obtained IRB approval, you should clearly state this in the paper.
    - We recognize that the procedures for this may vary significantly between institutions and locations, and we expect authors to adhere to the NeurIPS Code of Ethics and the guidelines for their institution.
    - For initial submissions, do not include any information that would break anonymity (if applicable), such as the institution conducting the review.

16. **Declaration of LLM usage**

    Question: Does the paper describe the usage of LLMs if it is an important, original, or non-standard component of the core methods in this research? Note that if the LLM is used only for writing, editing, or formatting purposes and does not impact the core methodology, scientific rigorousness, or originality of the research, declaration is not required.

    Answer: [NA]

    Justification:

    Guidelines:

    - The answer NA means that the core method development in this research does not involve LLMs as any important, original, or non-standard components.
    - Please refer to our LLM policy (https://neurips.cc/Conferences/2025/LLM) for what should or should not be described.